doi:10.1111/j.1558-5646.2011.01374.x

# LINEAGE DIVERSIFICATION AND MORPHOLOGICAL EVOLUTION IN A LARGE-SCALE CONTINENTAL RADIATION: THE NEOTROPICAL OVENBIRDS AND WOODCREEPERS (AVES: FURNARIIDAE)

**Elizabeth P. Derryberry,[1] Santiago Claramunt,[1] Graham Derryberry,[2] R. Terry Chesser,[3] Joel Cracraft,[4] Alexandre Aleixo,[5] Jorge Pérez-Emán,[6,7] J. V. Remsen, Jr.,[1] and Robb T. Brumfield[1,8]**

*[1]Museum of Natural Science and Department of Biological Sciences, Louisiana State University, Baton Rouge, Louisiana 70803*

*[2]BioComputing Asheville, 289 Lynn Cove Rd, Asheville, North Carolina 28803*

*[3]USGS Patuxent Wildlife Research Center, National Museum of Natural History, Smithsonian Institution, P.O. Box 37012, Washington, DC 20013*

*[4]Department of Ornithology, American Museum of Natural History, Central Park West at 79th St., New York, New York 10024*

*[5]Coordenação de Zoologia, Museu Paraense Emílio Goeldi, Caixa Postal 399, CEP 66040–170, Belém, Pará, Brazil*

*[6]Instituto de Zoología y Ecología Tropical, Universidad Central de Venezuela, Av. Los Ilustres, Los Chaguaramos, Apartado Postal 47058, Caracas 1041-A, Venezuela*

*[7]Colección Ornitológica Phelps, Apartado 2009, Caracas 1010-A, Venezuela*

*[8]E-mail: brumfld@lsu.edu*

Received September 28, 2010
Accepted April 30, 2011

**Patterns of diversification in species-rich clades provide insight into the processes that generate biological diversity. We tested different models of lineage and phenotypic diversification in an exceptional continental radiation, the ovenbird family Furnariidae, using the most complete species-level phylogenetic hypothesis produced to date for a major avian clade (97% of 293 species). We found that the Furnariidae exhibit nearly constant rates of lineage accumulation but show evidence of constrained morphological evolution. This pattern of sustained high rates of speciation despite limitations on phenotypic evolution contrasts with the results of most previous studies of evolutionary radiations, which have found a pattern of decelerating diversity-dependent lineage accumulation coupled with decelerating or constrained phenotypic evolution. Our results suggest that lineage accumulation in tropical continental radiations may not be as limited by ecological opportunities as in temperate or island radiations. More studies examining patterns of both lineage and phenotypic diversification are needed to understand the often complex tempo and mode of evolutionary radiations on continents.**

**KEY WORDS:** **Morphological Evolution, Phylogenetics, Adaptive Radiation.**

A central aim of evolutionary biology is to understand the historical processes driving species diversification. Both the fossil record and recent molecular phylogenetic studies that address the tempo of diversification typically yield a pattern of early, rapid cladogenesis followed by a decline in diversification rate (Stanley 1973; Harmon et al. 2003; Kadereit et al. 2004; Ruber and Zardoya 2005; Kozak et al. 2006; McKeena and Farrell 2006; McPeek 2008; Phillimore and Price 2008; Gavrilets and Losos 2009), although not every radiation shows density-dependent diversification (Alfaro et al. 2009a; Esselstyn et al. 2009; Slater et al. 2010). A common interpretation of a decline in diversification is that ecological opportunity facilitated an initial burst of speciation into new adaptive zones but then diversification rate declined as niches filled over time (Gavrilets and Vose 2005; Rabosky and Lovette 2008a). This inference of process from pattern is based on the ecological theory of adaptive radiations, which hypothesizes that ecological opportunity at first fuels but then limits radiations, predicting a pattern of diversity-dependent diversification and a slowdown over time in adaptive trait evolution (Simpson 1944; Schluter 2000). The process of increased competition for limited niches and phenotypic and genomic constraints on trait evolution could explain a pattern of slowdown in the rate of diversification (e.g., Simpson 1953; Foote 1997). On the other hand, a recent study suggests that simple geographic speciation, without the intervention of niche processes, can also generate a pattern of declining speciation through time (Pigot et al. 2010). Clearly, additional studies of both lineage accumulation and trait evolution across taxonomic groups are needed to understand the range of processes underlying evolutionary radiations.

Our understanding of the processes driving diversification is incomplete. Most studies to date have used incomplete phylogenies. Missing species can yield a false pattern of decline in diversification rate over time (Nee et al. 1994; Nee 2001), potentially leading to an over-association of radiations with diversity-dependent diversification (Cusimano and Renner 2010). In addition, the majority of studies have focused on radiations that are highly spatially limited (e.g., on islands or in lakes) (Baldwin and Sanderson 1998; Lovette et al. 2002; Gillespie 2004; Losos and Thorpe 2004; Seehausen 2006). With their relatively simple geography and small areal extent, island and lake radiations may experience similar histories of initial high niche availability and low competition, followed by a filling of niches over time. In contrast, the ecological histories of continental radiations are likely much more complex and varied and may yield a different tempo and mode of diversification (Irschick et al. 1997; Barraclough et al. 1999). Because most biodiversity resides on continents (May 1994), understanding the processes underlying diversification in ecologically and historically complex continental biotas is critical. Of the continental radiations examined in detail (e.g., McPeek and Brown 2000; Kozak et al. 2006; Rabosky and Lovette 2008a), many occupy only a small portion of the continent on which they occur, and few exhibit the high morphological diversity and species richness that characterize island and lake radiations. Testing evolutionary models of diversification in densely sampled, ecomorphologically diverse, species-rich continental radiations is essential to understand fully the historical processes that produce high species richness and phenotypic diversity.

We tested models of lineage accumulation and phenotypic evolution in one of the most well-recognized and largest (293+ species) of avian continental radiations (Fitzpatrick 1982; James 1982; Remsen 2003): the Neotropical ovenbirds and woodcreepers (Furnariidae, sensu Sibley and Monroe 1990; Remsen et al. 2011). When compared to the seven other families in the infraorder Furnariides (Moyle et al. 2009), the Furnariidae is characterized by a high rate of cladogenesis and a high diversity in morphological traits associated with feeding behavior and locomotion (Claramunt 2010a). The Furnariidae also represent a truly continental radiation: 97% of currently recognized species and 100% of genera occur within South America (Remsen 2003). In contrast to most Neotropical groups, furnariids are a predominant component of the avifauna in nearly all terrestrial habitats in South America (Ridgely and Tudor 1994; Marantz et al. 2003; Remsen 2003). Furnariids are found from the snow line at over 5000 m in the Andes down to the richest bird communities in the world in lowland Amazonia, and from perpetually wet cloud forests to nearly rainless deserts. The prevalence of furnariids throughout the Neotropical landscape as well as their exceptional diversity make them a particularly appropriate group for investigating diversification at a continental scale (Haffer 1969; Fjeldså et al. 2005).

Many geological and ecological processes could affect the pattern of lineage accumulation in a radiation that spans both an entire continent and a time period including major climatic shifts (e.g., to a more arid climate $\sim$ 15 Ma; Pleistocene climatic cycles) and geological events (e.g., the uplift of the Northern Andes between 2 and 5 Ma). Here, we employ likelihood methods for detecting temporal shifts in diversification rates to provide insight into the underlying causes of diversification in this family. We assess the consistency of the best-fitting model with scenarios of a slowdown in lineage accumulation through time due to ecological constraints (Gavrilets and Vose 2005) or to stable geographic range dynamics (diversity-dependent models) (Pigot et al. 2010), with hypotheses of shifts in diversification rate associated with major geological and climatic events or evolution of key traits (a discrete change in rates), and with a hypothesis of constant rate of diversification (pure-birth and birth–death models). We also test models that allow both speciation and extinction rates to vary, because moderate levels of extinction may obliterate the signal of early rapid diversification (Rabosky and Lovette 2008b). We next test competing hypotheses for the tempo of

phenotypic evolution in the Furnariidae, including a slowdown in the rate of phenotypic evolution, a constraint on trait evolution toward selective peaks (an Ornstein–Uhlenbeck [OU] process) and a Brownian motion (BM) process. To distinguish these hypotheses, we use three approaches, including likelihood models of continuous trait evolution (Pagel 1999), a node-height test (Freckleton and Harvey 2006), and disparity through time plots (Harmon et al. 2003).

# Methods and Materials

## MOLECULAR DATA

We sampled 285 of the 293 recognized species (97%) and all 69 recognized genera in the Furnariidae (Table S1). For most species (89%), we sequenced two or more vouchered specimens to validate species identification or for calibration purposes, but we did not include the second individual in subsequent analyses. As outgroups, we included representatives of all closely related families in the infraorder Furnariides (Moyle et al. 2009): Formicariidae, Rhinocryptidae, Grallariidae, Conopophagidae, Melanopareiidae, and Thamnophilidae, as well as representatives of Tyrannidae and Tityridae.

We used standard methods to extract genomic DNA from pectoral muscle and to amplify and sequence six genes (see Material and Methods in Supporting information). For the majority of individuals, we amplified and sequenced three mitochondrial genes and one nuclear intron: *NADH dehydrogenase subunit 3* (ND3; 351 bp), *cytochrome oxidase subunit 2* (CO2; 684 bp), *NADH dehydrogenase subunit 2* (ND2; 1041 bp), and β-*fibrinogen intron 7* (Bf7; ∼840 bp). For at least one individual per genus, we also included a large portion of the single exons of the *recombination activating genes* RAG-1 (2904bp) and RAG-2 (1152bp). Most RAG sequences were obtained from Moyle et al. (2009). For three individuals for whom we were unable to amplify one of these genes (*Philydor pyrrhodes*, *Lochmias nematura*, and *Sittasomus griseicapillus*), we used a sequence obtained for another individual of the same species.

We edited sequences using Sequencher 4.6 (Gene Codes Corporation, Ann Arbor, MI) and aligned sequences manually using Mesquite version 2.6 (Maddison and Maddison 2009). The final alignment included 6954 base pairs and was deposited in TreeBASE (Study ID S11550). Protein-coding sequences were translated into amino acids to confirm the absence of stop codons and anomalous residues. Preliminary phylogenetic analysis suggested that Bf7 sequences for the tribe Synallaxini were probably not orthologous; therefore, we excluded these sequences from further analyses. These sequences may represent a pseudogene and were not deposited in GenBank. All remaining sequences were deposited in GenBank under accession numbers JF974355-JF975363.

## PARTITIONS AND SUBSTITUTION MODELS

We estimated the optimal partitioning regime using the strategy described in Li et al. (2008) to designate partitions based on their similarity in evolutionary parameters (see Methods and Materials in Supporting information). We determined that a fully partitioned dataset (16 partitions) was the optimal partition strategy for the concatenated dataset (Table S2).

We used model selection techniques to determine the best substitution model for each partition under the optimal partition regime. With the tree obtained in the primary maximum-likelihood analysis, we used PAUP (Swofford 2003) to obtain likelihood values for all substitution models featured in Modeltest 3.7 (Posada and Crandall 1998) and calculated values of the Bayesian information criterion (BIC) (Posada and Crandall 1998; Sullivan and Joyce 2005). We identified the GTR + Γ + I model as the best model for the majority of the partitions, and the HKY + Γ + I model as the best model for the first and second codon positions of RAG 1 and all three codon positions of RAG 2.

## PHYLOGENETIC INFERENCE

We conducted a joint estimation of topology and divergence times in a Bayesian framework in the program BEAST version 1.5.2 (Drummund and Rambaut 2007) under an uncorrelated lognormal model (UCLD) (Drummund et al. 2006). We unlinked substitution model, rate heterogeneity, and base frequencies across partitions. We used a Yule prior for tree shape and the default priors for the substitution model and relaxed clock parameters. A UPGMA tree was used as the starting tree. No restrictions were placed on the topology so that topological uncertainty was factored into the divergence date estimates. Because furnariid fossils are rare, relatively recent, and of uncertain relationships (Claramunt and Rinderknecht 2005), we used biogeographic events to place priors on the age of the root and on the divergence times of the most recent common ancestor (tMRCA) of 12 sets of taxa (see Methods and Materials in Supporting information).

To optimize the Markov chain Monte Carlo (MCMC) operators, we performed incrementally longer runs and adjusted the scale factors for the operators as suggested by the BEAST output. Once scale factors stabilized, we ran analyses for a total of 150 million generations across seven independent runs. Using Tracer 1.5 (Drummund and Rambaut 2007), we determined that replicate analyses converged, and all parameters met benchmark effective sample size values (>200). We identified and discarded the burn-in. Converged runs were combined in LogCombiner (Drummund and Rambaut 2007) and used to estimate the posterior distributions of topologies and divergence times as well as the maximum clade credibility (MCC) tree.

## DIVERSIFICATION ANALYSES

We performed all analyses in R (R-Development-Core-Team 2008) using the Ape (Paradis et al. 2004), Geiger (Harmon et al. 2008), and Laser (Rabosky 2006) libraries. We used the MCC tree after excluding both the outgroup and ingroup samples used solely for calibration purposes (final included $n = 285$).

We used maximum-likelihood methods to compare models of lineage diversification and chose the best model using AIC. Using functions in the Laser library, we fit the following models of diversification: pure-birth (PB), birth–death (BD), Yule model with two rates (Y2R), linear (DDL) and exponential (DDX) diversity-dependent diversification, and three models that varied either speciation (SPVAR), extinction (EXVAR) or both (BOTHVAR) through time (Rabosky 2006; Rabosky and Lovette 2008b). We compared the fit of the best rate-variable model and best rate-constant model by computing the test statistic:

$$\Delta\text{AIC} = \text{AIC}_{\text{constant}} - \text{AIC}_{\text{Variable,}}$$

where $\text{AIC}_{\text{constant}}$ is the AIC score of the best rate-constant model and $\text{AIC}_{\text{variable}}$ is the AIC score of the best rate-variable model. A positive $\Delta$AIC implies that the rate-variable model fits the data better than the rate-constant model. To avoid conditioning our results, we determined the distribution of $\Delta$AIC over the posterior distribution of trees sampled using MCMC. To test for any over fitting of the data, we simulated 5000 phylogenies under a rate-constant model and compared the fit of the best rate-constant and rate-variable models to this null distribution. We simulated these phylogenies with 293 tips dropping eight of those tips to reflect sampling in the furnariid phylogeny (285 species with eight missing taxa).

To test for lineage-specific shifts in diversification rates, we used the MEDUSA algorithm (Modeling Evolutionary Diversification Using Stepwise AIC), which fits a series of BD models with an increasing number of breakpoints (rate shifts), and estimated the maximum-likelihood values for each set of birth and death parameters (Alfaro et al. 2009b). The method then uses a forward selection and backward elimination procedure to determine the simplest model with the highest likelihood to describe the given set of branch lengths, age, and species richness data. The threshold for retaining additional rate shifts was an improvement in AIC score of 4 units or greater (Burnham and Anderson 2003).

Another way of investigating models of diversification is to analyze the relationship between clade age and clade size. Older clades have had more time to accumulate diversity than younger clades (Labandeira and Sepkoski 1993; McPeek and Brown 2007). However, this positive relationship between age and diversity may breakdown due to clade volatility (differential extinction of clades with high and low diversification rates) (Gilinsky 1994; Sepkoski 1998), among-lineage variance in diversification rates, or ecological constraints on clade growth (Ricklefs 2006). A strong correlation between clade age and clade size, on the other hand, suggests a constant model of diversification. To assess the relationship between clade age and size in furnariids, we compared the age and species richness of 63 monophyletic groups as determined by the MCC tree. These groups corresponded in most cases to currently recognized genera, except that we included six previously monotypic genera within other genera based on the results of our phylogenetic hypothesis. For the crown age of each clade, we used the mean estimated age from the posterior distribution of trees. For clade size, we counted the number of recognized species (including those not included in the molecular phylogeny, $n = 8$; Remsen et al. 2011). Using a generalized least squares model correcting for phylogeny (Freckleton et al. 2002), we tested the prediction that clade age and clade size are positively correlated. We ran this analysis both including and excluding monotypic genera.

Extinction can affect the pattern of lineage accumulation. Simulation studies suggest that extinction can remove the signature of an early-burst radiation (i.e., an initial high rate of diversification followed by a slowdown over time), particularly under scenarios of a decline in speciation rate with a background of high relative extinction (Rabosky and Lovette 2008b, 2009). We evaluated and compared maximum-likelihood estimates of relative extinction and 95% profile-likelihood confidence intervals from the BD, SPVAR, EXVAR, and BOTHVAR models and the MEDUSA analysis. Because estimating extinction from molecular phylogenies can be problematic, we also examined theoretical expectations for scenarios of declining net diversification with a background of high relative extinction. To examine this idea under realistic parameters, we generated expected LTT curves under three scenarios of declining diversification rate (20-fold, 10-fold, and fivefold decline) each with an identical high relative extinction rate ($\varepsilon = 0.82$ [i.e., the relative extinction rate of suboscines (Ricklefs et al. 2007)]). Curves are theoretical expectations from Nee et al. (1994). We found parameters that would result in (1) three different declines in net diversification rate under an identical $\varepsilon$ and (2) a total of 285 surviving lineages after one time unit ($t = 1$). The net diversification rate was modeled as $r(t) = \lambda_0 e^{-zt}(1 - \varepsilon)$ following Rabosky and Lovette (2009). The code used to run this analysis in R can be found in Supporting information (ExtinctionLTT.R).

## MORPHOLOGICAL EVOLUTION ANALYSES

To describe ecomorphological variation, we measured 11 variables that represent the size and shape of major functional modules of avian external anatomy: bill, wing, tail, and feet. We included measurements for all species in the phylogeny except *Asthenes luizae*. We measured an average of 4.2 specimens per species (range: 1–19). Only three species were represented by a single

specimen, and most were represented by more than three. Bill length was measured from the anterior border of the nostril to tip of the bill, and bill width and depth (vertically) at the level of the anterior border of the nostrils. We took three wing measurements, all from the carpal joint and without flattening the natural curvature of the closed wing: (1) wing length to the longest primary, as a general measure of wing extent; (2) wing length to the tenth primary, the most distal one in furnarioids, which is related to the shape of the wing tip; and (3) length to the first secondary feather, which represents the width of an open wing. Tail maximum and minimum length were taken from the base of the central rectrices to the longest and shortest rectrices, respectively. The third tail measurement, an index of tail width, was measured as the width of the central rectrix at its midlength. We measured tarsus length and hallux length (including the claw) as measures of leg length and foot size, respectively. All measurements were taken with a Mitutoyo Digimatic Point Caliper by the same person (S. Claramunt) and loaded directly into an electronic spreadsheet using an input interface. Morphometric data were deposited as an associated document file in Microsoft Excel format in MorphoBank (http://www.morphobank.org) as part of the Morphological Evolution of the Furnariidae project. All morphological variables were log-transformed so that the differences between observations in the logarithmic space are proportional to differences in the original space (Ricklefs and Travis 1980).

We used AICc to compare the fit of three models of continuous trait evolution (Pagel 1999): a random walk model (BM Model), a model of constrained trait evolution toward an optimum (OU Model), and a model of deceleration ($\delta < 1$) or acceleration ($\delta > 1$) of trait evolution through time (Delta Model). To account for intraspecific variation in trait values, we incorporated standard error when fitting each model.

We then ran a node height test, which tests for accelerations or decelerations in trait evolution, by comparing the independent contrasts (IC) for a trait with the respective node height (estimate of relative age) (Freckleton and Harvey 2006). For each trait, we calculated IC incorporating measurement error (Felsenstein 2008). We then summed IC values across traits for a composite IC. We obtained node heights from the MCC tree. Using a linear model, we tested the prediction from the ecological theory of adaptive radiations of a negative correlation between the absolute values of the independent contrasts and node height. A negative correlation would imply that species are dividing niche space more finely through time, consistent with a niche-filling model. To meet model assumptions, we used the Box–Cox method (R-Development-Core-Team 2008) to determine the most appropriate transformation of the IC values for a linear model. The best transformation was a power transformation, with values raised to the power of 0.2.

We measured the time course of morphological diversification using disparity-through-time (DTT) plots (Harmon et al. 2003). Disparity is the dispersion of points in multivariate space and is usually measured as the mean squared Euclidean distance among species. However, we used the total variance instead (Van Valen 1974). The total variance is closely related to the mean squared Euclidean distance (Pie and Weitz 2005) but allowed us to take measurement error into account. We partitioned the total variance into two components, intraspecific and interspecific, using a random effect one way ANOVA, and used only the interspecific variance for the analysis. We also calculated the expected total variance under a BM model of trait evolution at each time point based on 10,000 phylogenetic simulations. We estimated the Brownian rate for the simulations using function fitContinuous incorporating measurement error. We plotted the mean subclade disparity for the observed and simulated data against node age. We also calculated the morphological disparity index (MDI), which is the area between observed and simulated clade disparity curves in standardized axes (Harmon et al. 2003). To determine the probability of obtaining a negative MDI value when the true model is BM, we computed the MDI value between our data and each of 10,000 simulated datasets. Negative values of MDI indicate that disparity through time is less than predicted under BM and that most variation is partitioned as among basal clades. Such a pattern indicates that clades tend to occupy different regions of morphological space, which is a common feature of adaptively radiating lineages (Harmon et al. 2003). The code used to run this analysis in R can be found in Supporting information (Variance Through Time functions.R).

# Results

## PHYLOGENETIC INFERENCE

A joint estimation of topology and divergence times in a Bayesian framework in the program BEAST version 1.5.2 (Drummund and Rambaut 2007) yielded a phylogenetic estimate for the Furnariidae with good resolution and high nodal support (>80% of nodes with posterior probability >0.95; Figs. 1 and S1).

## LINEAGE DIVERSIFICATION

Lineage accumulation in the Furnariidae occurred at a constant rate during most of the 30 million year history of the radiation with a shift to a lower rate 1.7 million years ago (Fig. 2). A Yule model with two rates (Y2R) provided the best fit (rate 1 = 0.16 lineages/Ma, rate 2 = 0.05, shift point = 1.17 Ma) based on model selection using AIC. The best-fit rate-constant model was a PB model. When we compared the fit of these models ($\Delta$AIC) to the posterior distribution of furnariid phylogenies sampled using MCMC, we found a positive distribution, implying that the Y2R

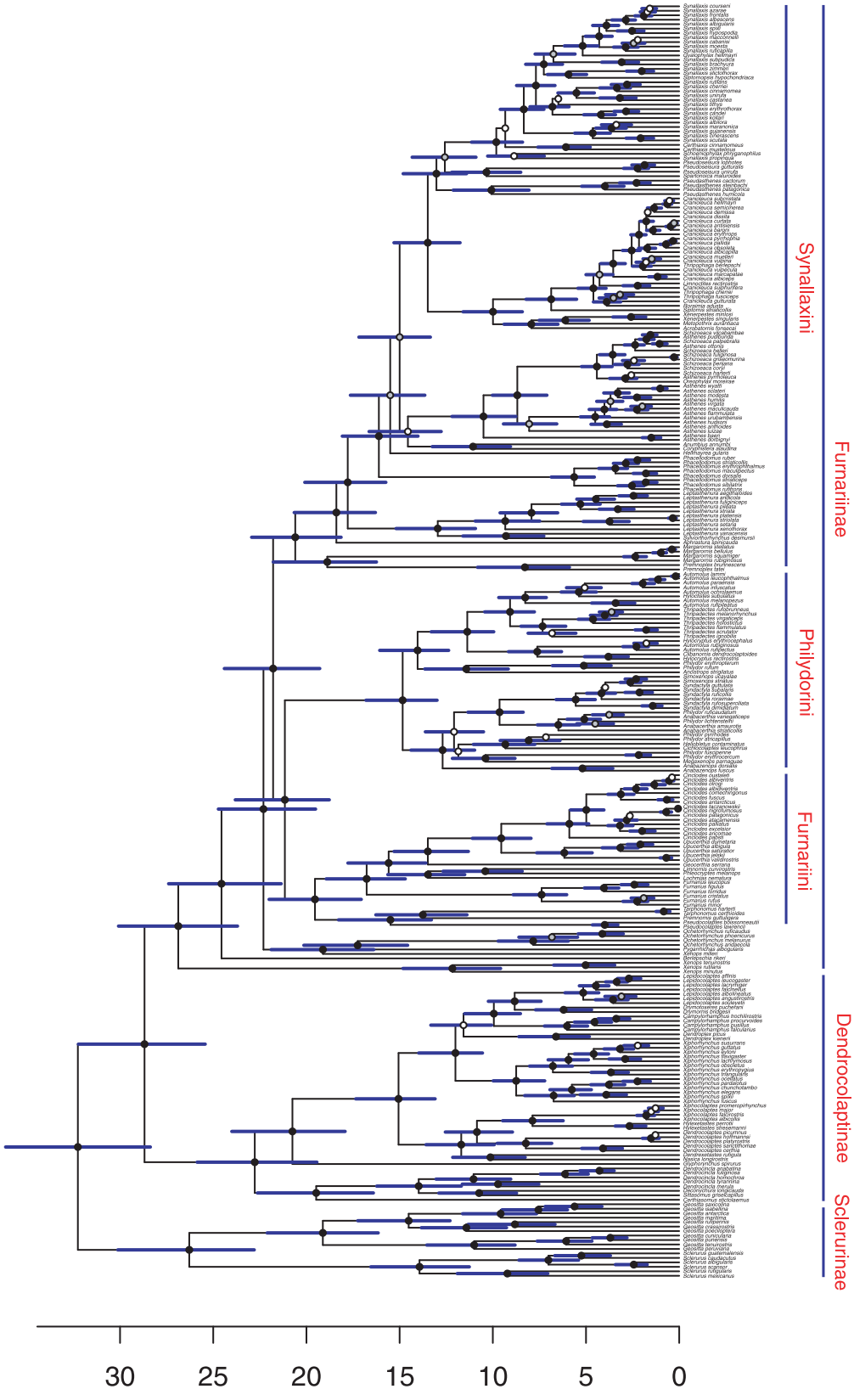


**Figure 1.** Bayesian estimate of phylogenetic relationships and divergence times among species of ovenbirds and woodcreepers (family Furnariidae) as inferred from a partitioned analysis of three mitochondrial and three nuclear genes. Bars at nodes indicate the 95% highest posterior density for the inferred divergence time estimates. The color of the circles at nodes indicates posterior probability support, > 95% (black), 95–75% (gray), <75% (white).

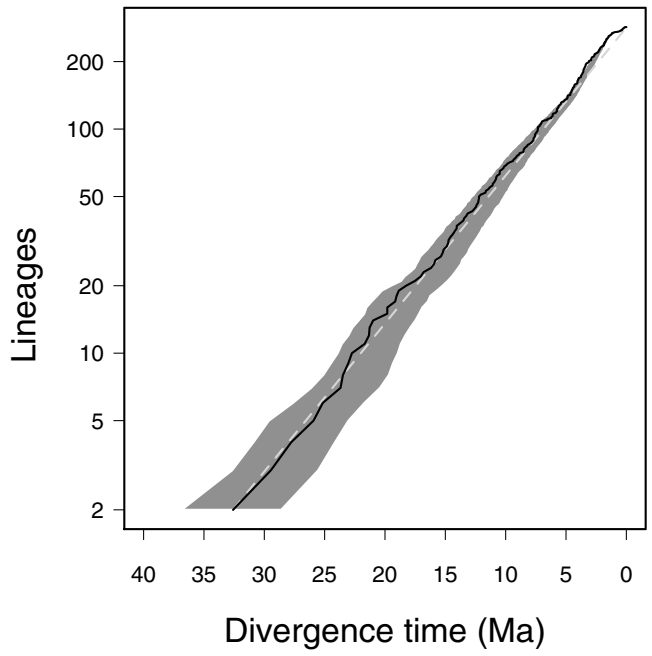


**Figure 2.** **Near-constant lineage accumulation over time in the Furnariidae radiation. The black line represents the number of lineages through time for the maximum clade credibility tree, and the gray shaded area is the 95% quantile on the number of lineages at any given time drawn from the posterior distribution of phylogenetic trees. The dashed line indicates the expected number of lineages under a constant-rate model of diversification with no extinction.**

**Table 1.** **Summary of diversification models fitted to the branching times derived from the Furnariidae phylogeny before (above the line) and after (below the line) truncating the tree at 1.17 Ma.**

| Model | Log likelihood | ΔAIC[1] |
|---|---|---|
| Yule-2-rate | 505.01 | 0 |
| Diversity-dependent, linear | 494.49 | 19.86 |
| Diversity-dependent, exponential | 492.58 | 22.86 |
| Pure-birth | 491.14 | 23.75 |
| Speciation decline | 492.37 | 25.28 |
| Birth-death | 491.14 | 25.74 |
| Both variable | 492.41 | 27.21 |
| Extinction-increase | 491.06 | 27.91 |
| Pure-birth | 476.47 | 0 |
| Birth-death | 476.59 | 1.76 |
| Yule-2-rate | 477.54 | 1.85 |
| Diversity-dependent, linear | 476.49 | 1.97 |
| Diversity-dependent, exponential | 476.47 | 2 |
| Speciation exponential decline | 476.61 | 3.73 |
| Extinction exponential increase | 476.58 | 3.77 |
| Variable speciation and extinction | 476.61 | 5.73 |

[1]**Difference in AIC scores between each model and the overall best-fit model.**

model fits the data better than a PB model. We then compared the fit of the Y2R and PB models to the null distribution from phylogenies simulated under a PB model. We found a distribution centered on zero with a long positive tail but with minimal overlap of the ΔAIC distribution tabulated from the posterior (Fig. S2). This result suggests that the Y2R model often provided a better fit than a PB model to simulated PB phylogenies. Despite this tendency to overfit the data, the Y2R model fits the observed data better than a PB model. After truncating the tree at the time of the rate shift, a rate-constant model received the strongest support (lower AIC indicates better model fit: PB AIC = –951; Y2R AIC = –949). All other models tested, including diversity-dependent diversification, received lower support (Table 1).

When we allowed rates of speciation and extinction to vary among lineages using the MEDUSA algorithm, we found strong support for two rate shifts from the background diversification rate ($r = \lambda - \mu = 0.1$; $\varepsilon = \mu/\lambda = 2.2 \times 10^{-05}$): one shift near the base of the Furnariinae approximately 23 Ma ($r = 0.16$; $\varepsilon = 2.5 \times 10^{-08}$), and a second shift near the base of the genus *Cranioleuca* approximately 3.5 Ma ($r = 0.58$; $\varepsilon = 2.5 \times 10^{-08}$).

We found a significant and positive relationship between genus age and species richness in the Furnariidae (phylogenetic GLS (Freckleton et al. 2002): including monotypic genera—$n = 63$, $R^2 = 0.57$, $F = 80.5$, $P < 9.5 \times 10^{-13}$; excluding monotypic genera—$n = 36$, $R^2 = 0.15$, $F = 5.8$, $P < 0.02$; Fig. S3). This correlation indicates that factors such as niche saturation or limits to clade size have not erased the signal of increased diversity over time (Rabosky 2009).

Maximum-likelihood estimates of extinction under a BD model indicate that extinction rates were orders of magnitude lower than speciation rates (relative extinction $\varepsilon = \mu/\lambda = 0$ [95% CI: 0, 0.105]). All other likelihood models that accounted for varying speciation and extinction rates (SPVAR, EXVAR, BOTHVAR) and for nonuniform processes (MEDUSA) provided estimates of extinction rates within this confidence interval. Low levels of extinction are unlikely to mask the signature of early burst radiations. Due to the difficulty of estimating extinction from molecular phylogenies, we also examined theoretical expectations for LTT curves in the context of declining rates of diversification and high relative extinction. When the decline in diversification is high (20- or 10-fold), the signal of early, rapid diversification is still apparent, even under high relative extinction (Fig. S4). When the decline in diversification is low (fivefold) under high relative extinction, then the result is a curve very similar to that seen under constant speciation with increasing extinction (i.e., an upturn in the number of lineages toward the present [Rabosky and Lovette 2008b]). None of these theoretical curves resemble the furnariid LTT curve, making it unlikely that the true pattern of diversification is one of declining speciation under high relative extinction.

**Table 2.** Summary of ΔAIC (difference between each model and the overall best-fit model) for three models of trait evolution for each morphological trait.

| Morphological character | BMM[1] | DM[2] | OUM[3] |
|---|---|---|---|
| Wing length to the longest primary | **0** | 1.9 | 1.9 |
| Wing length to the tenth primary (wing tip shape) | **0** | 1.6 | 1.4 |
| Wing width | **0** | 1.0 | 0.6 |
| Tail maximum length | **0** | 1.8 | 1.6 |
| Tail minimum length | 0.4 | 0 | **0** |
| Tail width | 1.4 | 0.4 | **0** |
| Bill length | **0** | 0.7 | 2.0 |
| Bill width | **0** | 1.2 | 2.0 |
| Bill depth | **0** | 2.0 | 2.0 |
| Tarsus length | **0** | 0.4 | 0.5 |
| Hallux length | 0.8 | **0** | 0.8 |

[1]Brownian Motion Model.
[2]Delta Model.
[3]Ornstein–Uhlenbeck Model.

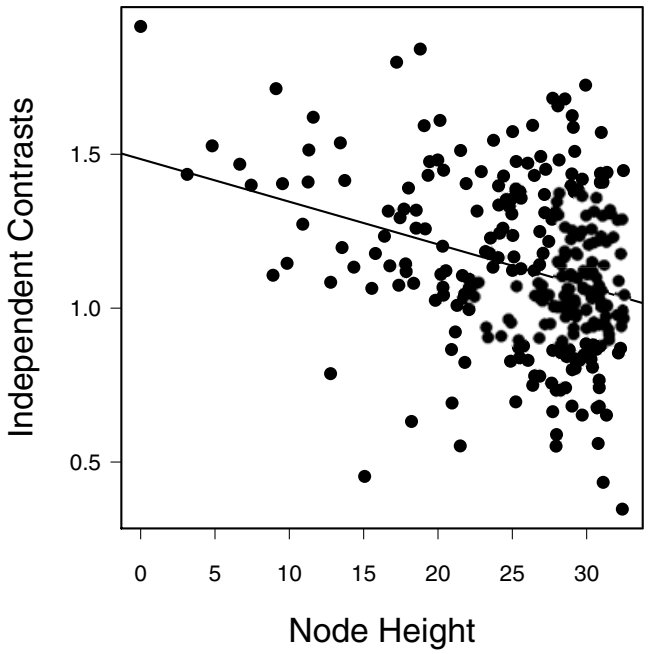


**Figure 3.** A negative relationship between node height and independent contrasts for morphological traits. Absolute value of the composite independent contrasts describing morphological space compared to the height (relative age) of the corresponding node. The negative relationship between node height and independent contrasts is significant ($n = 280$, $t = -5.44$, $P < 1 \times 10^{-7}$). The solid line is the best-fit line. Independent contrasts were power-transformed to stabilize variance. Lower contrast values indicate that paired comparisons are relatively similar in morphology. Node height is the distance from the root to a given node, such that the height of the root is zero.

### MORPHOLOGICAL EVOLUTION

We found that a BM model provided the best fit for eight of the 11 traits. A model with a constraint on trait evolution toward an optimum (OU) described trait evolution best for two traits (tail minimum length and tail width), and the Delta model provided the best fit for one trait (hallux length). The difference in AICc values between these alternative models and the BM model were very low (ΔAICc < 2 units), suggesting that the OU and Delta models do not provide a substantially better fit than a BM model (Table 2).

We next used the node height test to detect accelerations or decelerations in trait evolution over time. Using this test, we found a significant negative relationship between the composite index of independent contrast scores and node height ($t = -5.44$, $P < 1\times 10^{-07}$; Fig. 3). This negative relationship held across individual traits. These results suggest that furnariids are dividing morphological space more finely through time, consistent with a niche-filling model.

The time course of morphological diversification indicated that relative disparity through time for morphological traits was less than that predicted under a BM model (Fig. 4). Supporting this qualitative assessment, our analysis yielded a negative MDI value (MDI = –0.156). There were no MDI values greater than zero, indicating that a BM process cannot explain morphological evolution in the furnariids. Values of disparity less than predicted under BM suggest that most variation is partitioned as among basal clade differences, indicating that basal clades tend to occupy different regions of morphological space.

## *Discussion*

### LINEAGE DIVERSIFICATION

The tempo of lineage accumulation in the Furnariidae was nearly constant through time (Fig. 2) apart from a few rate shifts near the base and near the tips of the furnariid phylogeny. Model selection and the MEDUSA analysis identified three discrete rate shifts. One of these shifts was a rate decrease that occurred recently (∼1 Ma) relative to the age of the radiation (∼33 Ma) and could be detected across the entire phylogeny. We determined that this rate shift is not a spurious result of the Yule two-rate model overfitting the data. Therefore, this shift may represent an artifact of missing phylotaxa or a real decrease in net diversification due to a geological or climatic event. In this family, many biological species comprise more than one divergent evolutionary lineage (cf. Tobias et al. 2008; e.g., Sanín et al. 2009). Many missing young lineages could yield a false signature of a recent shift to a lower rate of diversification. If true, then including these cryptic lineages may erase the recent rate shift. Another explanation for this pattern is that a real decrease in net diversification rate

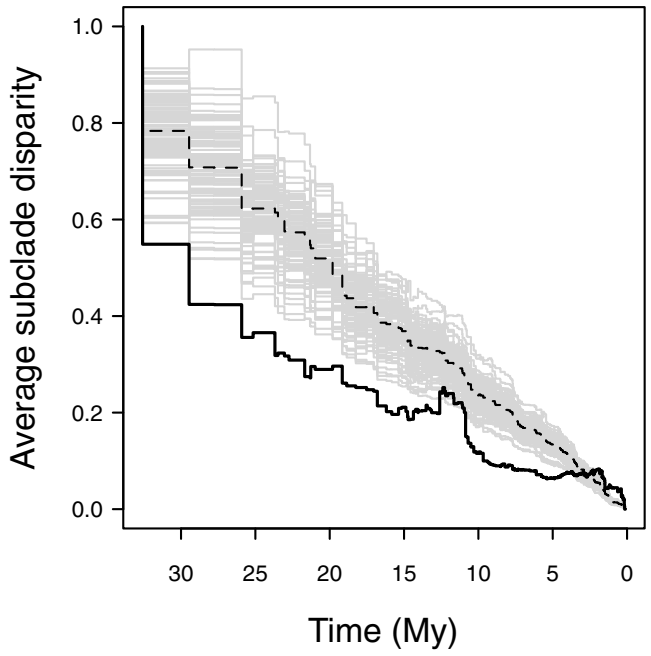


**Figure 4. Relative disparity through time (DTT) for morphological traits was less than that predicted under a Brownian motion model. Disparity values closer to 1 indicate that most variation is found within subclades and values closer to 0 indicate that variation is partitioned among subclades relative to the entire clade. Solid line indicates actual disparity; dashed line indicates median expected disparity and gray lines indicate expected disparity for a sample of 100 simulations based on a Brownian motion model.**

occurred approximately 1 Ma due to dramatic fluctuations in climate during the Pleistocene. At this time, distinguishing these two scenarios is not possible. However, it is important to note that neither diversity-dependent diversification nor an exponential increase in extinction can explain this recent decrease in the rate of diversification, because both models received low support (Table 1). Together, our results suggest that lineage accumulation occurred at a constant rate for most of the history of the Furnariidae.

When we allowed clades to vary in speciation and extinction rates using MEDUSA, we found evidence for at least two lineage-specific rate shifts. Both shifts were significant increases in diversification rate. The first occurred approximately 23 Ma (range: 17 – 27 Ma) near the base of the radiation containing most of the subfamily Furnariinae. Fjeldså et al. (2005) suggested that changes in cranial kinesis at the base of the Furnariinae may be in part responsible for high rates of diversification in this group. Ancestral character reconstructions or trait-dependent diversification analyses (Maddison et al. 2007) are needed to test this hypothesis. Of the three subfamilies, Furnariinae has the highest species richness, and at least one hypothesis (Irestedt et al. 2009) suggests that the radiation of this lineage was propelled by a major climatic shift to a more arid climate in South America beginning approximately 15 Ma (Zachos et al. 2001). Species in this subfamily tend to occupy more open environments and aridification creates more open environments, thus potentially facilitating speciation in this group. Our results do not support this hypothesis, because the shift in diversification rate appears to have occurred prior to the shift in climate. However, ruling out an association between diversification and climate shifts is difficult, because estimates of the timing of both often have large confidence intervals.

A second increase in diversification occurred approximately 3.5 Ma along the stem of a clade containing most, but not all, of the species in the genus *Cranioleuca.* Previous work has noted extremely low levels of interspecific genetic divergence in this species-rich group, suggesting rapid and recent diversification (García-Moreno et al. 1999), but the driving force behind this is not immediately apparent. Rapid diversification in this group does not appear to be the result of a key morphological or behavioral innovation (Claramunt 2010b). Species in this genus are typical furnariines that do not differ significantly in foraging behavior, nesting behavior, or morphology. However, plumage evolution can occur rapidly in this genus (Remsen 1984) and different traits seem to change independently from each other (Maijer and Fjeldsa 1997; Claramunt 2002). These two factors can produce multiple combinations of plumage characters in short evolutionary time. If some of these plumage traits confer reproductive isolation, then this could explain rapid speciation in this clade.

## CLADE AGE VERSUS CLADE SIZE

For lineages diversifying at a nearly constant rate, older clades are expected to have had more time to accumulate diversity than younger clades (Labandeira and Sepkoski 1993; McPeek and Brown 2007). This process should generate a positive relationship between clade age and size. If species diversity were limiting diversification in the furnariids, then we would expect clade size to achieve a state of equilibrium, weakening the relationship between clade age and size. Instead, we found a significant, positive relationship between clade age and species richness, consistent with our finding of a nearly constant rate of lineage accumulation in the furnariids.

Several empirical studies on higher taxa have found a negative or no relationship between clade age and clade diversity (Magallon and Sanderson 2001 [Angiosperm clades]; Ricklefs 2006 [Avian tribes]; McPeek and Brown 2007 [Mammalian orders and Teleost fish orders]; Rabosky 2010b [Ant genera]). The correlation between age and diversity may breakdown due to clade volatility (Gilinsky 1994; Sepkoski 1998), among-lineage rate variation, or ecological constraints. Rabosky (2009, 2010b) tested whether these factors could explain the breakdown in the relationship between clade age and size in higher taxa. His results suggested that only ecological constraints, rather than clade

volatility or variance in clade diversification rates, are a strong enough effect to disrupt the expected positive relationship between clade age and diversity. If ecological constraints are the primary factor reducing the correlation between clade age and size, then furnariids appear to be less constrained by ecological factors than other higher taxa examined to date.

## ROLE OF EXTINCTION

Extinction is of concern when evaluating lineage diversification because high levels of extinction can erase the signature of rapid initial lineage diversification (Rabosky and Lovette 2008b). We estimated a low level of relative extinction for furnariids ($\varepsilon = 0.10$), but estimates of extinction rates from molecular phylogenies can be incorrect (Rabosky 2010a). Estimating extinction from molecular phylogenies is problematic because BD models assume complete, resolved phylogenies and no constraints on clade growth. Simulation studies suggest that for phylogenetic trees with complete taxonomic sampling (in the case of the furnariids, 97% of species sampled), estimates of relative extinction are unbiased in the absence of among-lineage rate variation (Rabosky 2010a). As among-lineage rate variation increases in simulations, estimates of relative extinction become upwardly biased (Rabosky 2010a). Thus, our estimate of low relative extinction for the furnariids is more likely to be upwardly biased than too low an estimate. However, confidence intervals in these simulation studies are high, and it is possible that relative extinction in the furnariids is higher than we estimated.

Simulation studies suggest that moderate-to-high levels of extinction can remove the evidence of rapid early diversification followed by a slowdown (Rabosky and Lovette 2008b, 2009). A slowdown in diversification can occur via several different scenarios, including a decline in speciation, an increase in extinction, or both. In simulations of declining speciation with no extinction, lineage accumulation curves show the expected slowdown in diversification (Rabosky and Lovette 2008b). In simulations of increasing extinction under constant speciation, the number of lineages increases toward the present. This "pull of the present" can create an apparent excess of recent lineages. Thus, a slowdown in diversification due to increasing extinction through time yields a pattern of increasing diversification toward the present rather than a pattern of constant diversification. We do not find an upturn in the number of lineages in the furnariid LTT plot; instead, we find an LTT curve nearly indistinguishable from that expected under constant diversification (Fig. 2). This suggests that neither declining speciation under zero extinction nor increasing extinction under constant speciation can explain the pattern of furnariid diversification. This result is supported by model fitting in that neither the SPVAR nor the EXVAR (variable speciation or extinction through time) models received strong support. However, a more complex model of varying and nonuniform speciation and extinction rates could potentially generate a pattern nearly indistinguishable from a constant rate model.

There may be certain scenarios in which a decline in speciation coupled with a high level of relative extinction could yield a pattern of lineage accumulation difficult to differentiate from constant diversification. In simulations of a decline in speciation, the signature of the decline is reduced as the relative level of constant extinction is increased (Rabosky and Lovette 2009). Under relative extinction levels of 0 to 0.75, the signature of a decline in diversification is still apparent but less pronounced. And under extremely high relative extinction (0.99), there is an upturn in the number of lineages toward the present. However, relative extinction levels between 0.75 and 0.99 might result in a pattern similar to constant diversification. If furnariids have a high level of relative extinction, then it is possible that the true scenario of furnariid diversification is one of declining speciation with a high level of background extinction. However, none of the theoretical LTT curves generated under scenarios of declining diversification and high relative extinction rate ($\varepsilon = 0.82$ [e.g., estimated relative extinction rate in the suboscines (Ricklefs et al. 2007)]) resembled the furnariid LTT curve, making it unlikely that the true pattern of diversification is one of declining speciation under high relative extinction.

## MORPHOLOGICAL EVOLUTION

Theory suggests that as organisms diversify into new adaptive zones, morphological evolution should be rapid at first and then slow as ecological opportunities become limited (Simpson 1944). If morphological evolution in furnariids is a function of ecological opportunity, then we predicted that we would find support for (1) furnariids diversifying into new adaptive zones, (2) early and rapid morphological evolution followed by a significant slowdown, and (3) niche saturation. Consistent with the first prediction, the disparity through time plot indicated that furnariids partitioned morphological disparity among rather than within clades. This finding suggests that furnariid lineages evolved along distinct morphological trajectories through time, probably exploring different adaptive zones. Providing support for the third prediction, we found evidence that furnariids have divided morphological space more finely through time, as the absolute contrast in morphological trait values decreased from the root to the tips in the node height test. This pattern is usually indicative of niche saturation. However, model selection did not provide support for the second prediction of decelerating trait evolution (Delta $< 1$). Instead, evolution of most of the traits examined appears consistent with a BM process. Altogether, our results suggest that furnariids diversified early along different morphological trajectories and the difference among these trajectories (or adaptive zones) has become smaller over time, but morphological evolution has not slowed. Instead, traits appear to be evolving according to a random walk process.

The pattern of morphological evolution in furnariids is more consistent with an early burst of diversification, as found in *Dendroica* warblers (Rabosky and Lovette 2008a), than with a lineage experiencing nearly constant diversification through time. Partitioning of disparity among rather than within clades is more often associated with lineages undergoing early, rapid cladogenesis, whereas equal partitioning of disparity within and among clades is more often associated with lineages exhibiting constant diversification (Harmon et al. 2003). This pattern of association between disparity and diversity is often considered evidence that lineages exploring new adaptive zones undergo bursts of lineage diversification (Burbrink and Pyron 2010). We find evidence of furnariids exploring new adaptive zones, but not of an excess of early speciation events. Niche saturation is also more consistent with a radiation undergoing diversity-dependent diversification. For example, as the diversity of competing lineages present on an island increases, *Anolis* lizards divide morphological space more finely (Mahler et al. 2010). A study of the evolution of feeding adaptations in Old World leaf warblers (*Phylloscopus* spp.) also found evidence of niche saturation limiting phenotypic evolution (Freckleton and Harvey 2006). If speciation is linked to ecological opportunities, then niche saturation should be associated with a decline in speciation rate. However, in the furnariids, we find evidence of niche saturation but not of a decline in diversification. Only the likelihood models provided evidence of uniform morphological evolution with no evidence of limits on clade growth, consistent with a radiation undergoing constant lineage accumulation.

Inconsistency between disparity and diversity analyses could indicate either that morphological analyses are picking up a signature of early, rapid lineage accumulation that was not detected by the diversification analyses or that the pattern of disparity and diversity are not tightly linked in the furnariid radiation. As mentioned earlier, there are factors, such as moderate-to-high levels of extinction, that can erase the signature of early, rapid diversification (Rabosky and Lovette 2009). This signature might have disappeared from the phylogeny but remains apparent in the morphological data. A recent analysis of disparity and diversity in modern whales (Neoceti) also could not distinguish lineage diversification from a Yule model but found evidence of niche saturation and a negative MDI (Slater et al. 2010). This study concluded that the signature of an adaptive radiation might be retained in morphological traits even after it has been erased from the structure of a phylogeny. However, if this was the case in the Furnariidae, then we would have expected limitations on clade growth leading to a low correlation between clade age and size; instead, we found a significant correlation between clade age and size. This result does not provide evidence against ecological limits on lineage accumulation but does suggest that it is a less likely interpretation of the data. The furnariid radiation might instead exhibit real differences in patterns of disparity and diversity, indicating either that the furnariid radiation is on a trajectory to slow down but has not done so yet or that speciation is not linked tightly to ecological opportunities in this group.

Because the Furnariidae are an exceptional radiation, characterized by both a high rate of cladogenesis and high diversity in morphological traits (Claramunt 2010a), we predicted that this group would show signatures of an adaptive radiation (Gavrilets and Losos 2009), including a slowdown in lineage accumulation and in phenotypic evolution over time. Although we find some evidence of the latter, we did not find evidence of the former, which leads us to consider how the spatial and temporal distribution of ecological opportunities across radiations may affect patterns of lineage accumulation. Most island and lake radiations probably experienced one period of open niches that facilitated rapid speciation (Seehausen 2006; Gavrilets and Losos 2009). If these radiations were able to continue to colonize new areas, such as nearby islands, then a constant rate of diversification could be maintained via a series of new ecological opportunities. For example, the Southeast Asian shrew (*Crocidura*) radiation on the Southeast Asian archipelagos has a near-constant rate of lineage diversification that may be associated with its continued colonization of new islands (Esselstyn et al. 2009). However, in most island or lake radiations, once niches filled, diversification rate could only decline. For example, successive radiations of cichlids show early bursts and then declines in diversification (Seehausen 2006) as successive radiations of *Anolis* lizards show declines in phenotypic diversification (Mahler et al. 2010). In contrast, the Furnariidae span an entire continent and a time period including major climatic shifts and geological events; thus, they have experienced a series of ecological opportunities over time due to dynamic habitat and range changes.

Concurrent with the furnariid radiation in South America, dramatic geoclimatic changes, from the uplift of the Andes to the development of the Amazon riverine system, created abundant opportunities for both geographic and ecological speciation. Geological studies suggest that the central and northern Andes rose in a series of pulses over the past 25 million years (Gregory-Wodzicki 2000), creating new vegetation zones and changing the organization of the Amazon and Paraná river basins several times (Hoorn et al. 1995; Figueiredo et al. 2009). These biogeographic events created multiple barriers to dispersal as well as a series of new habitats into which furnariids could radiate. This continuous creation of new barriers and niches may have facilitated near-constant diversification in the furnariid radiation in spite of constraints on phenotypic evolution. As diversification patterns and ecological histories of continental radiations are examined with the attention given to island radiations, continental radiations will likely prove to be complex and varied in their tempo and mode of lineage and phenotypic diversification.

## ACKNOWLEDGMENTS

We thank M. E. Alfaro, R. E. Ricklefs, C. D. Cadena, and two anonymous reviewers for helpful comments on earlier drafts of the manuscript. We thank numerous collectors, including C. M. Milensky, and institutions for providing tissue samples (see Table S1) and C. Burney, G. Bravo, C. D. Cadena, A. Cuervo, J. Maley, and L. Naka for sequence data for this project. G. Bravo, J. M. Brown, J. W. Brown, L. Harmon, C. Heibl, W. Pfeiffer, J. McCormack, D. Rabosky, A. Rambaut, and M. Tingley provided code, analysis assistance, and discussion concerning analyses. This research was supported in part by NSF grants DBI-0400797 and DEB-0543562 to RTB, NSF AToL grant EAR-0228693 to JC, Frank M. Chapman (AMNH) and NSF-RTG (Univ. of Arizona) postdoctoral fellowships and a faculty/research small grant (Univ. of Arizona) to RTC, CNPq (Brazil) grants 310593/2009–3, 574008/2008–0, and 476212/2007–3 to AA, and a Sigma Xi Grant-in-Aid of Research to SC. Any use of trade, product, or firm names is for descriptive purposes only and does not imply endorsement by the U.S. Government.

## LITERATURE CITED

Alfaro, M. E., C. D. Brock, B. L. Banbury, and P. C. Wainwright. 2009a. Does evolutionary innovation in pharyngeal jaws lead to rapid lineage diversification in labrid fishes? BMC Evol. Biol. 9:255.

Alfaro, M. E., F. Santini, C. Brock, H. Alamillo, A. Dornburg, D. L. Rabosky, G. Carnevale, and L. J. Harmon. 2009b. Nine exceptional radiations plus high turnover explains species diversity in jawed vertebrates. Proc. Natl. Acad. Sci. USA 106:13410–13414.

Baldwin, B. G., and M. J. Sanderson. 1998. Age and rate of diversification of the Hawaiian silversword alliance (Compositae). Proc. Natl. Acad. Sci. USA 95:9402–9406.

Barraclough, T. G., J. E. Hogan, and A. P. Vogler. 1999. Testing whether ecological factors promote cladogenesis in an group of tiger beetles (Coleoptera: Cicindelidae). Proc. R. Soc. Lond. B 266:1061–1067.

Burbrink, F. T., and R. A. Pyron. 2010. How does ecological opportunity influence rates of speciation, extinction and morphological diversification in New World ratsnakes (Tribe Lampropeltini)? Evolution 64:934–943.

Burnham, K. P., and D. R. Anderson. 2003. Model selection and multimodel inference, a practical information-theoretic approach. Springer, New York.

Claramunt, S. 2002. Variación geogr´fica en Cranioleuca pyrrhophia y el límite con Cranioleuca obsoleta (Furnariidae). Ornitología Neotropical 13:255–266.

———. 2010a. Discovering exceptional diversifications at continental scales: the case of the endemic families of Neotropical suboscine passerines. Evolution 64:2004–2019.

———. 2010b. Testing models of biological diversification: morphological evolution and cladogenesis in the Neotropical Furnariidae (Aves: Passeriformes). Department of Biological Sciences. Louisiana State Univ., Baton Rouge, LA.

Claramunt, S., and A. Rinderknecht. 2005. A new fossil furnariid from the Pleistocene of Uruguay, with remarks on nasal type, cranial kinetics, and relationships of the extinct genus *Pseudoseisuropsis*. Condor 107:114–127.

Cusimano, N., and S. S. Renner. 2010. Slowdowns in diversification rates from real phylogenies may not be real. Syst. Biol. 59:458–464.

Drummund, A. J., and A. Rambaut. 2007. BEAST: Bayesian evolutionary analysis by sampling trees. BMC Evol. Biol. 7:214.

Drummund, A. J., S. Y. W. Ho, M. J. Phillips, and A. Rambaut. 2006. Relaxed phylogenetics and dating with confidence. PLoS Biol. 4:e88.

Esselstyn, J. A., R. M. Timm, and R. M. Brown. 2009. Do geological or climatic processes drive speciation in dynamic archipelagos? The tempo and mode of diversification in Southeast Asian shrews. Evolution 63:2595–2610.

Felsenstein, J. 2008. Comparative methods with sampling error and within-species variation: contrasts revisited and revised. Am. Nat. 171: 713–725.

Figueiredo, F., C. Hoorn, P. van der ven, and E. Soares. 2009. Late Miocene onset of the Amazonian River and the Amazon deep-sea fan: evidence from the Foz do Amazonas Basin. Geology 37:619–622.

Fitzpatrick, J. W. 1982. Reviews: Taxonomy and geographical distribution of the Furnariidae (Aves, Passeriformes) by Charles Vaurie. Auk 99:810–813.

Fjeldså, J., M. Irestedt, and P. G. P. Ericson. 2005. Molecular data reveal some major adaptational shifts in the early evolution of the most diverse avian family, the Furnariidae. J. Ornithol. 146:1–13.

Foote, M. 1997. The evolution of morphological diversity. Annu. Rev. Ecol. Evol. Syst. 28:129–152.

Freckleton, R. P., and P. H. Harvey. 2006. Detecting non-Brownian trait evolution in adaptive radiations. PLoS Biol. 4:2104–2111.

Freckleton, R. P., P. H. Harvey, and M. Pagel. 2002. Phylogenetic analysis and comparative data: a test and review of evidence. Am. Nat. 160: 712–726.

García-Moreno, J., P. Arctander, and J. Fjeldsa. 1999. A case of rapid diversification in the neotropics: phylogenetic relationships among Cranioleuca spinetails (Aves, Furnariidae). Mol. Phylogenet. Evol. 12:273–281.

Gavrilets, S., and A. Vose. 2005. Dynamic patterns of adaptive radiation. Proc. Natl. Acad. Sci. USA 102:18040–18045.

Gavrilets, S., and J. B. Losos. 2009. Adaptive radiation: contrasting theory with data. Science 323:732–737.

Gilinsky, N. L. 1994. Volatility and the Phanerozoic decline of background extinction intensity. Paleobiology 20:445–458.

Gillespie, R. 2004. Community assembly through adaptive radiation in Hawaiian spiders. Science 303:356–359.

Gregory-Wodzicki, K. M. 2000. Uplift history of the central and northern Andes: A review. GSA Bulletin 112:1091–1105.

Haffer, J. 1969. Speciation in Amazonian forest birds. Science 165:131–137.

Harmon, L. J., J. A. Schulte, A. Larson, and J. B. Losos. 2003. Tempo and mode of evolutionary radiation in iguanian lizards. Science 301:961–964.

Harmon, L. J., J. T. Weir, C. D. Brock, R. E. Glor, and W. Challenger. 2008. GEIGER: investigating evolutionary radiations. Bioinformatics 24:129–131.

Hoorn, C., J. Guerrero, G. A. Sarmiento, and M. A. Lorente. 1995. Andean tectonics as a cause for changing drainage patterns in Miocene northern South America. Geology 23:237–240.

Irestedt, M., J. Fjeldså, L. Dalen, and P. G. P. Ericson. 2009. Convergent evolution, habitat shifts and variable diversification rates in the ovenbird-woodcreeper family (Furnariidae). BMC Evol. Biol. 9:268.

Irschick, D. J., L. J. Vitt, P. A. Zani, and J. B. Losos. 1997. A comparison of evolutionary radiations in mainland and Caribbean *Anolis* lizards. Ecology 78:2191–2203.

James, F. C. 1982. The ecological morphology of birds: a review. Ann. Zool. Fenn. 19:265–276.

Kadereit, J. W., E. M. Griebeler, and H. P. Comes. 2004. Quaternary diversification in European alpine plants: pattern and process. Philos. Trans. R. Soc. Lond. B 359:265–274.

Kozak, K. H., D. W. Weisrock, and A. Larson. 2006. Rapid lineage accumulation in a non-adaptive radiation: phylogenetic analysis of diversification rates in eastern North American woodland salamanders (Plethodontidae: *Plethodon*). Proc. R. Soc. Lond. B 273:539–546.

Labandeira, C. C., and J. J. Sepkoski. 1993. Insect diversity in the fossil record. Science 261:310–315.

Li, C., G. Lu, and G. Orti. 2008. Optimal data partitioning and a test case for Ray-finned fishes (Actinopterygii) based on ten nuclear loci. Syst. Biol. 57:519–539.

Losos, J. B., and R. S. Thorpe. 2004. Evolutionary diversification of Caribbean *Anolis* lizards. Pp. 322–324 *in* U. Dieckmann, J. A. Doebeli, J. A. J. Metz, and D. Tautz, eds. Adaptive speciation. Cambridge Univ. Press, Cambridge, England.

Lovette, I. J., E. Bermingham, and R. E. Ricklefs. 2002. Clade-specific morphological diversification and adaptive radiation in Hawaiian songbirds. Proc. R. Soc. Lond. B 269:37–42.

Maddison, W. P., and D. R. Maddison. 2009. Mesquite: a modular system for evolutionary analysis. Available at http://mesquite.project.org(Accessed May 4, 2008).

Maddison, W. P., P. E. Midford, and S. P. Otto. 2007. Estimating a binary character's effect on speciation and extinction. Syst. Biol. 56:701–710.

Magallon, S. M., and M. J. Sanderson. 2001. Absolute diversification rates in angiosperm clades. Evolution 55:1762–1780.

Mahler, D. L., L. J. Revell, R. E. Glor, and J. B. Losos. 2010. Ecological opportunity and the rate of morphological evolution in the diversification of Greater Antillean anoles. Evolution 64:2731–2745.

Maijer, S., and J. Fjeldsa. 1997. Description of a new Cranioleuca spinetail from Bolivia and a ''leapfrog pattern'' of geographic variation in the genus. Ibis 139:607–616.

Marantz, C. A., A. Aleixo, L. R. Bevier, and M. A. T. Patten, Jr. 2003. Pp. 358–447 *in* J. del Hoyo, A. Elliott, and D. A. Christie, eds. Family Dendrocolaptidae (Woodcreepers).Lynx Edicions, Barcelona.

May, R. M. 1994. Biological diversity: differences between land and sea. Philos. Trans. R. Soc. Lond. B 343:105–111.

McKeena, D. D., and B. D. Farrell. 2006. Tropical forests are both evolutionary cradels and museums of leaf beetle diversity. Proc. Natl. Acad. Sci. USA 103:10947–10951.

McPeek, M. A. 2008. The ecological dynamics of clade diversification and community assembly. Am. Nat. 172:E270-E284.

McPeek, M. A., and J. M. Brown. 2000. Building a regional species pool: diversification of the *Enallagma* damselflies in eastern North America. Ecology 81:904–920.

———. 2007. Clade age and not diversification rate explains species richness among animal taxa. Am. Nat. 169:E97–E106.

Moyle, R. G., R. T. Chesser, R. T. Brumfield, J. G. Tello, D. J. Marchese, and J. Cracraft. 2009. Phylogeny and phylogenetic classification of the antbirds, ovenbirds, woodcreepers, and allies (Aves: Passeriformes: Furnariides). Cladistics 25:386–405.

Nee, S. 2001. Inferring speciation rates from phylogenies. Evolution 55:661–668.

Nee, S., E. C. Holmes, R. M. May, and P. H. Harvey. 1994. Extinction rates can be estimated from molecular phylogenies. Philos. Trans. R. Soc. Lond. B. 344:77–82.

Pagel, M. 1999. Inferring the historical patterns of biological evolution. Nature 401:877–884.

Paradis, E., J. Claude, and K. Strimmer. 2004. APE: analyses of phylogenetics and evolution in R language. Bioinformatics 20:289–290.

Phillimore, A. B., and T. D. Price. 2008. Density-dependent cladogenesis in birds. PLoS Biol. 6:e71.

Pie, M. R., and J. S. Weitz. 2005. A null model of morphospace occupation. Am. Nat. 166:E1–E13.

Pigot, A. L., A. B. Phillimore, I. P. F. Owens, and C. D. L. Orme. 2010. The shape and temporal dynamics of phylogenetic trees arising from geographic speciation. Syst. Biol. 59:660–673.

Posada, D., and K. A. Crandall. 1998. Modeltest: testing the model of DNA substitution. Bioinformatics 14:817–818.

R-Development-Core-Team. 2008. R: A language and environment for statistical computing. Available at http://www.R-project.org. R Foundation for Statistical Computing, Vienna, Austria.

Rabosky, D. L. 2006. LASER: A maximum likelihood toolkit for detecting temporal shifts in diversification rates from molecular phylogenies. Evol. Bioinform. 2:247–250.

———. 2009. Ecological limits on clade diversification in higher taxa. Am. Nat. 173:662–674.

———. 2010a. Extinction rates should not be estimated from molecular phylogenies. Evolution 64:1816–1824.

———. 2010b. Primary controls on species richness in higher taxa. Syst. Biol. 59:634–645.

Rabosky, D. L., and I. J. Lovette. 2008a. Density-dependent diversification in North American wood warblers. Proc. R. Soc. Lond. B 275:2363–2371.

———. 2008b. Explosive evolutionary radiations: decreasing speciation or increasing extinction through time? Evolution 62:1866–1875.

———. 2009. Problems detecting density-dependent diversification on phylogenies: reply to Bokma. Proc. R. Soc. Lond. B 276:995–997.

Remsen, J. V. 1984. Geographic variation, zoogeography, and possible rapid evolution in some *Cranioleuca* spinetails (Furnaridae). Wilson Bulletin 96:515–523.

———. 2003. Family Furnariidae (ovenbirds). Pp. 162–201,302–315 *in* J. Hoyo, A. Elliot, and D. A. Christie, eds. Handbook of the birds of the world. Lynx Edicions, Barcelona.

Remsen, J. V., C. D. Cadena, A. Jaramillo, M. Nores, J. F. Pacheco, M. B. Robbins, T. S. Schulenberg, F. G. Stiles, D. Stotz, and K. J. Zimmer. 2011. A classification of the bird species of South America. American Ornithologists' Union. Available at http://www.museum.lsu.edu/∼Resen/SACCBasline.html

Ricklefs, R. E. 2006. Global variation in the diversification rate of passerine birds. Ecology 87:2468–2478.

Ricklefs, R. E., and J. Travis. 1980. A morphological approach to the study of avian community organization. Auk 97:321–338.

Ricklefs, R. E., J. B. Losos, and T. M. Townsend. 2007. Evolutionary diversification of clades of squamate reptiles. J. Evol. Biol. 20:1751–1762.

Ridgely, R. S., and G. Tudor. 1994. The Birds of South America, Vol. II: The suboscine passerines: Ovenbirds.

Ruber, L., and R. Zardoya. 2005. Rapid cladogenesis in marine fishes revisted. Evolution 59:1119–1127.

Sanín, C., C. D. Cadena, J. M. Maley, D. A. Lijtmaer, P. L. Tubaro, and R. T. Chesser. 2009. Paraphyly of *Cinclodes fuscus* (Aves: Passeriformes: Furnariidae): implications for taxonomy and biogeography. Mol. Phylogenet. Evol. 53:547–555.

Schluter, D. 2000. The ecology of adaptive radiation. Oxford Univ. Press, Oxford.

Seehausen, O. 2006. African cichlid fish: a model system in adaptive radiation research. Proc. R. Soc. Lond. B 273:1987–1998.

Sepkoski, J. J. 1998. Rates of speciation in the fossil record. Philos. Trans. R. Soc. Lond. B 353:315–326.

Sibley, C. G., and B. L. J. Monroe. 1990. Distribution and taxonomy of birds of the world. Yale Univ. Press, New Haven, CT.

Simpson, G. G. 1944. Tempo and mode in evolution. Columbia Univ. Press, New York.

———. 1953. The major features of evolution. Columbia Univ. Press, New York.

Slater, G. J., S. A. Price, F. Santini, and M. E. Alfaro. 2010. Diversity versus disparity and the radiation of modern cetaceans. Proc. R. Soc. Lond. B 277:3097–3104.

Stanley, S. M. 1973. Effects of competition on rates of evolution with special reference to bivalve molluscs and mammals. Syst. Zool. 22:486–506.

Sullivan, J., and P. Joyce. 2005. Model selection in phylogenetics. Annu. Rev. Ecol. Evol. Syst. 36:445–466.

Swofford, D. L. 2003. PAUP*. Phylogenetic Analysis Using Parsimony (*and other methods). Sinauer Associates, Sunderland, MA.

Tobias, J. A., J. M. Bates, S. J. Hackett, and N. Seddon. 2008. Comment on "The latitudinal gradient in recent speciation and extinction rates of birds and mammals". Science 319:901c.

Van Valen, L. 1974. Multivariate structural statistics in natural history. J. Theor. Biol. 45:235–347.

Zachos, J., M. Pagani, L. Sloan, E. Thomas, and K. Billups. 2001. Trends, rhythms, and abberations in global climate 65 Ma to present. Science 292:686–693.

Associate Editor: M. Alfaro

## *Supporting Information*

The following supporting information is available for this article:

**Figure S1.** Maximum clade credibility (MCC) tree of the Furnariidae. MCC tree inferred using BEAST version 1.5.2.

**Figure S2.** Distribution of $\Delta$AIC test statistic calculated from the posterior distribution of furnariid phylogenies sampled using MCMC (black) and from a null distribution of phylogenies simulated under a constant-rate model (gray).

**Figure S3.** Species richness increases with clade age.

**Figure S4.** Expected LTT curves under an identical high relative extinction rate ($\varepsilon = 0.82$) and different net diversification rates (20fold, 10fold and fivefold decline from left to right) with 285 surviving lineages.

**Table S1.** Accession numbers and locality information for samples included in the Furnariidae phylogeny.

**Table S2.** Statistics for selection of the best partitioning strategy.Supporting Information may be found in the online version of this article.

Supporting Information may be found in the online version of this article.

**Supporting Methods and Materials**

*Molecular data*

Using the Qiagen DNeasy kit, genomic DNA was extracted from 25 mg of pectoral muscle following the manufacturer's protocol. Amplifications were performed using the polymerase chain reaction (PCR). Primers used for amplification and sequencing were L10755/H11151 (Chesser 1999) for ND3, NF3COII/SCTRCOII (Sanín et al. 2009; Claramunt et al. 2010) for CO2, FIB-BI7U/BI7L (Prychitko and Moore 1997) and FIBI7-397U/439L (Chesser 2004) for Bf7, and H6313/L5758 (Johnson and Sorenson 1998), L5215 (Hackett 1996), and H5766 (Brumfield et al. 2007) for ND2. RAG-1 and RAG-2 genes were amplified and sequenced using multiple primer pairs (Groth and Barrowclough 1999; Barker et al. 2002; Barker et al. 2004).

In a 20 μl total volume, PCR amplifications contained approximately 60 ng of genomic template DNA, 50 mM KCl, 10mM Tris-HCl, 1.5 mM MgCl, 0.5 mM dNTPs, 0.75 μM of each external primer, and 0.08 U Promega *Taq*. The thermocycling program consisted of an initial denaturing step (94°C for 2 min) followed by 35 cycles of 94°C for 1 min, a 30s annealing step (ND3, 46°C; CO2, 55°C; Bf7, 55°C; ND2, 50°C), and a 72°C extension step for 1 min. The program ended with a final 72°C extension step for 3 min. We purified PCR products using PEG precipitation, eluted in 12.5 μl 10mM Tris, and sequenced using the ABI Prism cycle sequencing protocol (Applied Biosystems Inc.) modified for ¼ - ½ reactions (depending on the length of the gene). Sequencing reactions

were purified using Sephadex ® G-50 and 400 μl 96 well filter plates. Cycle-sequencing products were visualized on an ABI 3100 Genetic Analyzer.

*Partitions and substitution models*

We estimated the optimal partitioning regime using the strategy described in Li *et al.* (2008) to designate partitions based on their similarity in evolutionary parameters. The data were fully partitioned (a different partition for each position of each coding gene (15) and the nuclear intron) and each of the 16 data blocks was optimized independently under a GTR+Γ model using the ML method in RAxML. We analyzed the similarity among the data blocks based on their estimated parameter values, including substitution rates, base composition (empirical proportions), and the gamma parameter. The resulting UPGMA was used as a visual guide to propose seven partitioning strategies. We ran analyses using all data in two partitions (mtDNA codon position 3 versus everything else), three partitions (mtDNA-1&2, mtDNA-3, nuclear DNA), seven partitions (mtDNA-1, mtDNA-2, mtDNA-3, RAG1&2-1, RAG1&2-2, RAG1&2-3, Bf7), nine partitions (mtDNA-1, mtDNA-2, CO2-3, ND3-3, ND2-3, RAG1&2-1, RAG1&2-2, RAG1&2-3, BF7), 11 partitions (CO2-1, ND3-1, ND2-1, mtDNA-2, CO2-3, ND3-3, ND2-3, RAG1&2-1, RAG1&2-2, RAG1&2-3, BF7), 14 partitions (CO2-1, ND3-1, ND2-1, CO2-2, ND3-2, ND2-2, CO2-3, ND3-3, ND2-3, RAG1&2-1, RAG1&2-2, RAG1-3, RAG2-3, BF7), and fully partitioned (see above). We then used RAxML to obtain likelihood values for each partition strategy for both GTR+ Γ and GTR+ Γ+I models and calculated values of the small sample size version of the Akaike Information Criterion (AICc).

*Phylogenetic inference: use of biogeographic events for calibration*

As with most passerines, furnariid fossils are rare, relatively recent, and of uncertain relationships (Claramunt and Rinderknecht 2005). Therefore, we used biogeographic events for calibration. We placed a prior distribution on the age of the root: the split between the Tyrannoidea and the Furnarioidea. Barker et al. (2004) estimated nodal ages of the order Passeriformes using penalized likelihood (PL) (Sanderson 2002), with the basal divergence of *Acanthisitta* calibrated by the sundering of New Zealand from Antarctica (Cracraft 2001). This calibration yielded a divergence date of Tyrannoidea from Furnarioidea of 61 ± 2.8 Ma (Barker et al. 2004). This date is comparable to the 63 Ma derived by Sibley and Ahlquist (Sibley and Ahlquist 1990). We allowed for bi-directional uncertainty in this event and placed a normal prior distribution on the age of the root with a mean of 61 and a standard deviation of 2.8.

We also placed priors on the divergence times of the most recent common ancestor (tMRCA) of 12 sets of taxa using two biogeographic events: the closure of the Panamanian Isthmus and the uplift of the Eastern Cordillera of the northern Andes. The Isthmus of Panama was completed in the Pliocene (Duque-Caro 1990) but might not have had an immediate effect on speciation events (Ho 2007). Therefore, we allowed for bi-directional uncertainty in this event and modeled "Isthmus" calibration points as normal distributions with a mean of 3.0 million years and a standard deviation of 0.5 million years, following Weinstock et al. (2005). The uplift of the Eastern Andean Cordillera occurred over an extended period of time, but paleobotanical data suggest that elevations

were no more than 40% of current height from the middle Miocene until approximately 4 Ma (Gregory-Wodzicki 2000). A rapid increase in elevation occurred between 2 and 5 Ma, when modern elevations were reached. To reflect the timing of the uplift, we modeled "Andean" calibration points as lognormal distributions with a mean of 1.3 and a standard deviation of 0.9, which translates to a median age of 3.6 Ma with a 95% age interval of 0.8 to 16 Ma. This distribution allows for some bidirectional uncertainty and reflects our hypothesis that the uplift of the Eastern Andean Cordillera had a functional role for furnariid evolution over an extended period of time prior to reaching modern elevations.

We used seven "Isthmus" and five "Andean" tMRCAs. The "Isthmus" tMRCAs were chosen as clade-pairs in which one clade's current range is restricted to Central America west of central Panama, whereas the other clade's current range is restricted to South America or to Central America east of central Panama. These MRCAs corresponded to the following clades: (1) *Synallaxis candei* and *S. erythrothorax*, (2) *Cranioleuca subcristata*, *C. hellmayri, C. semicinerea, C. demissa,* and *C. dissita*, (3) *Lepidocolaptes lacrymiger*, *L. leucogaster,* and *L. affinis*, (4) *Margarornis rubiginosus*, *M. squamiger, M. bellulus,* and *M. stellatus*, (5) *Thripadectes melanorhynchus* and *T. rufobrunneus*, (6) *Anabacerthia variegaticeps variegaticeps* and *A. v. temporalis*, and (7) *Pseudocolaptes lawrencii lawrencii*, *P. l. johnsoni,* and *P. boissonneautii*. The "Andean" tMRCAs were chosen as northern South American clade-pairs in which one clade's current range is trans-Andean (west of the Andes) but east of central Panama, and the other clade's current range is cis-Andean (east of the Andes). All taxa used in these analyses are

restricted to mid- to low-elevation habitats. These tMRCAs included: (1) *Hyloctistes subulatus assimilis* and *H. s. subulatus*; (2) *Automolus rubiginosus watkinsi, A. r. nigricauda*, *A. r. saturatus*, *A. rufipectus*, and *Hylocryptus erythrocephalus*; (3) *Philydor erythrocercum* and *P. fuscipenne*; (4) *Xenops minutus littoralis*, X. *m. minutus*, and *X. m. remoratus*; and (5) *Dendrocolaptes certhia certhia*, *D. c. concolor*, and *D. sanctithomae*.

## REFERENCES


Barker, F. K., G. F. Barrowclough, and J. G. Groth. 2002. A phylogenetic hypothesis for passerine birds: taxonomic and biogeographic implications of an analysis of nuclear DNA sequence data. Proc. R. Soc. Lond. B Biol. Sci. 269:295-308.

Barker, F. K., A. Cibois, P. Schikler, J. Feinstein, and J. Cracraft. 2004. Phylogeny and diversification of the largest avian radiation. Proc. Natl. Acad. Sci. U. S. A. 101:11040-11045.

Brumfield, R. T., J. G. Tello, Z. A. Cheviron, M. D. Carling, N. Crochet, and K. V. Rosenberg. 2007. Phylogenetic conservatism and antiquity of a tropical specialization: Army-ant-following in the typical antbirds (Thamnophilidae). Mol. Phylogenet. Evol. 45:1-13.

Chesser, R. T. 1999. Molecular systematics of the rhinocryptid genus *Pteroptochos*. Condor 101:439-446.

Chesser, R. T. 2004. Molecular systematics of New World suboscine birds. Mol. Phylogenet. Evol. 32:11-24.

Claramunt, S., E. Derryberry, R. T. Chesser, A. Aleixo, and R. T. Brumfield. 2010. Polyphyly of *Campylorhamphus*, and description of a new genus for *C. pucherani* (Dendrocolaptinae). The Auk 127:430-439.

Claramunt, S., and A. Rinderknecht. 2005. A new fossil furnariid from the Pleistocene of Uruguay, with remarks on nasal type, cranial kinetics, and relationships of the extinct genus *Pseudoseisuropsis*. Condor 107:114-127.

Cracraft, J. 2001. Avian evolution, Gondwana biogeography, and the Cretaceous-Tertiary mass extinction event. Proc. R. Soc. Lond. B Biol. Sci. 268B:459-469.

Duque-Caro, H. 1990. Neogene stratigraphy, paleoceanography and paleobiogeography in northwest South America and the evolution of the Panama seaway. Palaeogeogr. Palaeoclimatol. Palaeoecol. 77:203-234.

Gregory-Wodzicki, K. M. 2000. Uplift history of the central and northern Andes: A review. GSA Bulletin 112:1091-1105.

Groth, J. G., and G. F. Barrowclough. 1999. Basal divergence in birds and the phylogenetic utility of the nuclear RAG-1 gene. Mol. Phylogenet. Evol. 12:115-123.

Hackett, S. J. 1996. Molecular phylogenetics and biogeography of tanagers in the genus *Ramphocelus* (Aves). Mol. Phylogenet. Evol. 5:368-382.

Ho, S. Y. W. 2007. Calibrating molecular estimates of substitution rates and divergence times in birds. J. Avian Biol. 38:409-414.

Johnson, K. P., and M. D. Sorenson. 1998. Comparing molecular evolution in two mitochondrial protein coding genes (Cytochrome *b* and ND2) in the dabbling ducks (Tribe: Anatini). Mol. Phylogenet. Evol. 10:82-94.

Li, C., G. Lu, and G. Orti. 2008. Optimal data partitioning and a test case for Ray-finned fishes (Actinopterygii) based on ten nuclear loci. Syst. Biol. 57:519-539.

Prychitko, T. M., and W. S. Moore. 1997. The utility of DNA sequences of an intron from the B-fibrinogen gene in phylogenetic analysis of woodpeckers (Aves: Picidae). Mol. Phylogenet. Evol. 8:193-204.

Sanderson, M. J. 2002. Estimating absolute rates of molecular evolution and divergence times: a penalized likelihood approach. Mol. Biol. Evol. 19:101-109.

Sanín, C., C. D. Cadena, J. M. Maley, D. A. Lijtmaer, P. L. Tubaro, and R. T. Chesser. 2009. Paraphyly of *Cinclodes fuscus* (Aves: Passeriformes: Furnariidae): Implications for taxonomy and biogeography. Mol. Phylogen. Evol. 53:547-555.

Sibley, C. G., and J. E. Ahlquist. 1990. Phylogeny and classification of birds: a study in molecular evolution. Yale University Press, New Haven, CT.

Weinstock, J., E. Willerslev, A. Sher, W. Tong, S. Y. W. Ho, D. Rubenstein, J. Storer, J. Burns, L. Martin, C. Bravi, A. Prieto, D. Froese, E. Scott, L. Xulong, and A. Cooper. 2005. Evolution, systematics, and phylogeography of Pleistocene horses in the New World: a molecular perspective. PLoS Biol. 3:e241.

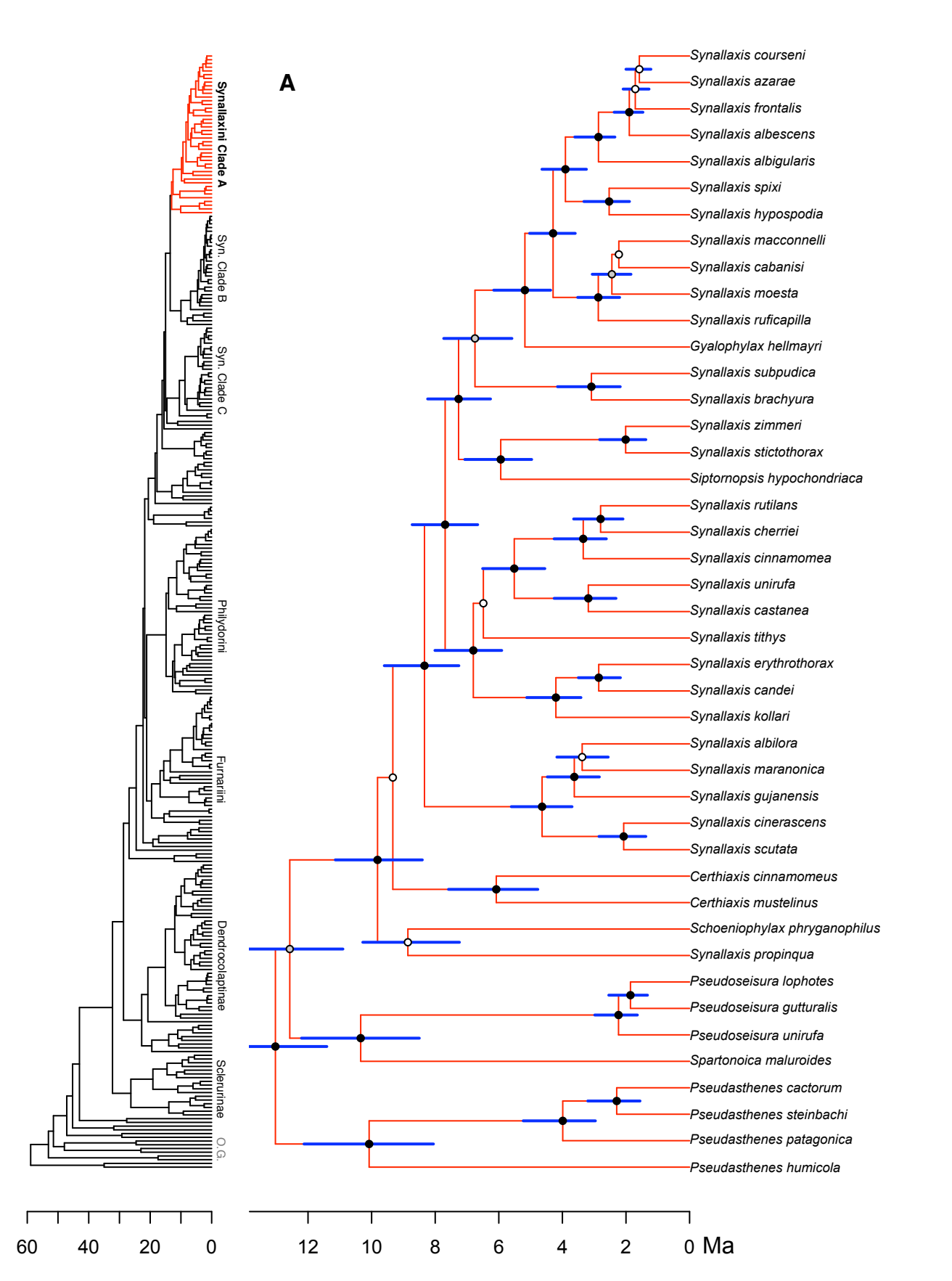
A
Synallaxini Clade A
Syn. Clade B
Syn. Clade C
Philydorini
Furnariini
Dendrocolaptinae
Sclerurinae
O.G.
Synallaxis courseni
Synallaxis azarae
Synallaxis frontalis
Synallaxis albescens
Synallaxis albigularis
Synallaxis spixi
Synallaxis hypospodia
Synallaxis macconnelli
Synallaxis cabanisi
Synallaxis moesta
Synallaxis ruficapilla
Gyalophylax hellmayri
Synallaxis subpudica
Synallaxis brachyura
Synallaxis zimmeri
Synallaxis stictothorax
Siptornopsis hypochondriaca
Synallaxis rutilans
Synallaxis cherriei
Synallaxis cinnamomea
Synallaxis unirufa
Synallaxis castanea
Synallaxis tithys
Synallaxis erythrothorax
Synallaxis candei
Synallaxis kollari
Synallaxis albilora
Synallaxis maranonica
Synallaxis gujanensis
Synallaxis cinerascens
Synallaxis scutata
Certhiaxis cinnamomeus
Certhiaxis mustelinus
Schoeniophylax phryganophilus
Synallaxis propinqua
Pseudoseisura lophotes
Pseudoseisura gutturalis
Pseudoseisura unirufa
Spartonoica maluroides
Pseudasthenes cactorum
Pseudasthenes steinbachi
Pseudasthenes patagonica
Pseudasthenes humicola
60
40
20
0
12
10
8
6
4
2
0
Ma

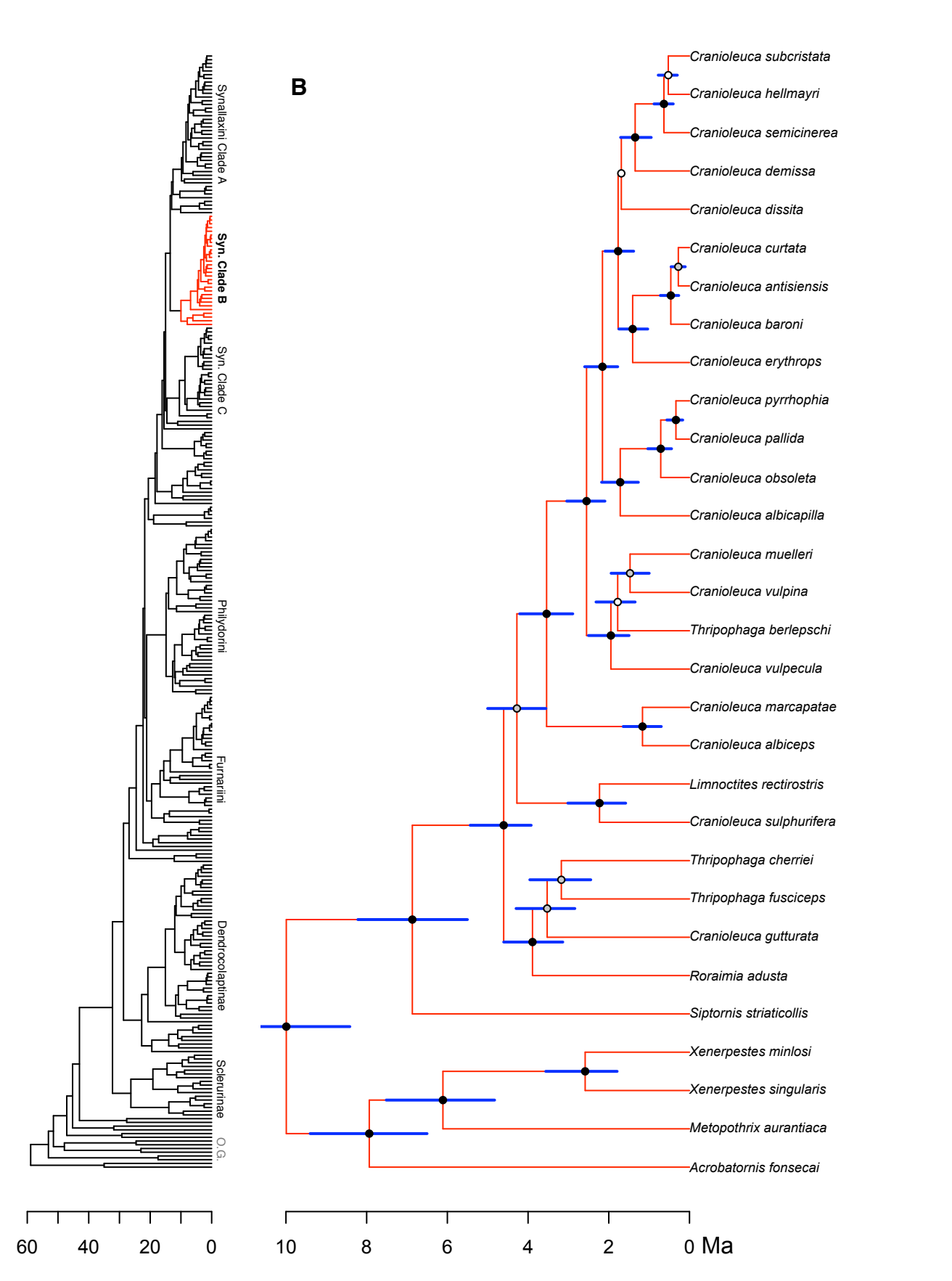
B
Synallaxini Clade A
Syn. Clade B
Syn. Clade C
Philydorini
Furnariini
Dendrocolaptinae
Sclerurinae
O.G.
Cranioleuca subcristata
Cranioleuca hellmayri
Cranioleuca semicinerea
Cranioleuca demissa
Cranioleuca dissita
Cranioleuca curtata
Cranioleuca antisiensis
Cranioleuca baroni
Cranioleuca erythrops
Cranioleuca pyrrhophia
Cranioleuca pallida
Cranioleuca obsoleta
Cranioleuca albicapilla
Cranioleuca muelleri
Cranioleuca vulpina
Thripophaga berlepschi
Cranioleuca vulpecula
Cranioleuca marcapatae
Cranioleuca albiceps
Limnoctites rectirostris
Cranioleuca sulphurifera
Thripophaga cherriei
Thripophaga fusciceps
Cranioleuca gutturata
Roraimia adusta
Siptornis striaticollis
Xenerpestes minlosi
Xenerpestes singularis
Metopothrix aurantiaca
Acrobatornis fonsecai
60
40
20
0
10
8
6
4
2
0 Ma

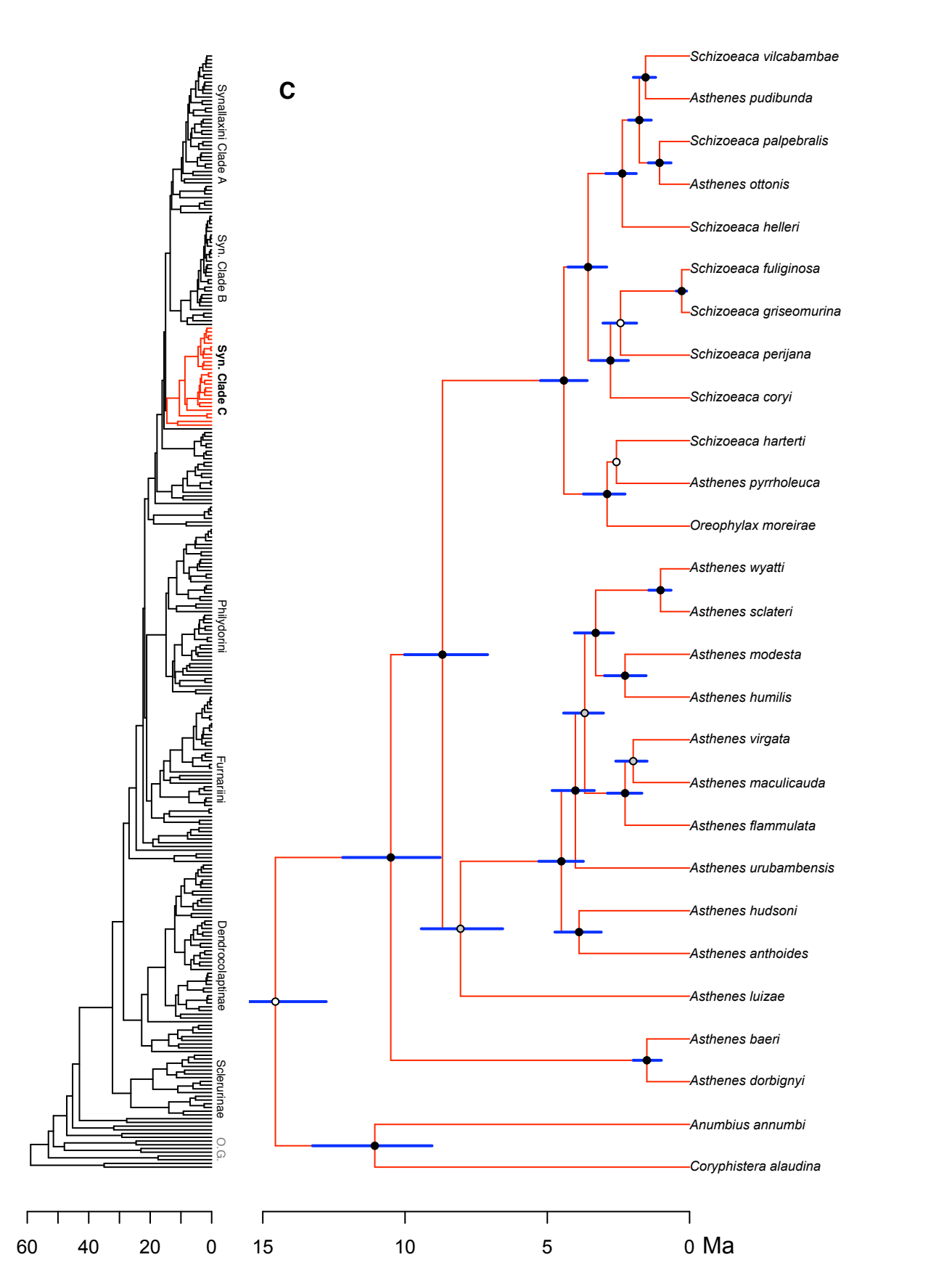
C
Synallaxini Clade A
Syn. Clade B
Syn. Clade C
Philydorini
Furnariini
Dendrocolaptinae
Sclerurinae
O.G.
Schizoeaca vilcabambae
Asthenes pudibunda
Schizoeaca palpebralis
Asthenes ottonis
Schizoeaca helleri
Schizoeaca fuliginosa
Schizoeaca griseomurina
Schizoeaca perijana
Schizoeaca coryi
Schizoeaca harterti
Asthenes pyrrholeuca
Oreophylax moreirae
Asthenes wyatti
Asthenes sclateri
Asthenes modesta
Asthenes humilis
Asthenes virgata
Asthenes maculicauda
Asthenes flammulata
Asthenes urubambensis
Asthenes hudsoni
Asthenes anthoides
Asthenes luizae
Asthenes baeri
Asthenes dorbignyi
Anumbius annumbi
Coryphistera alaudina
60
40
20
0
15
10
5
0 Ma

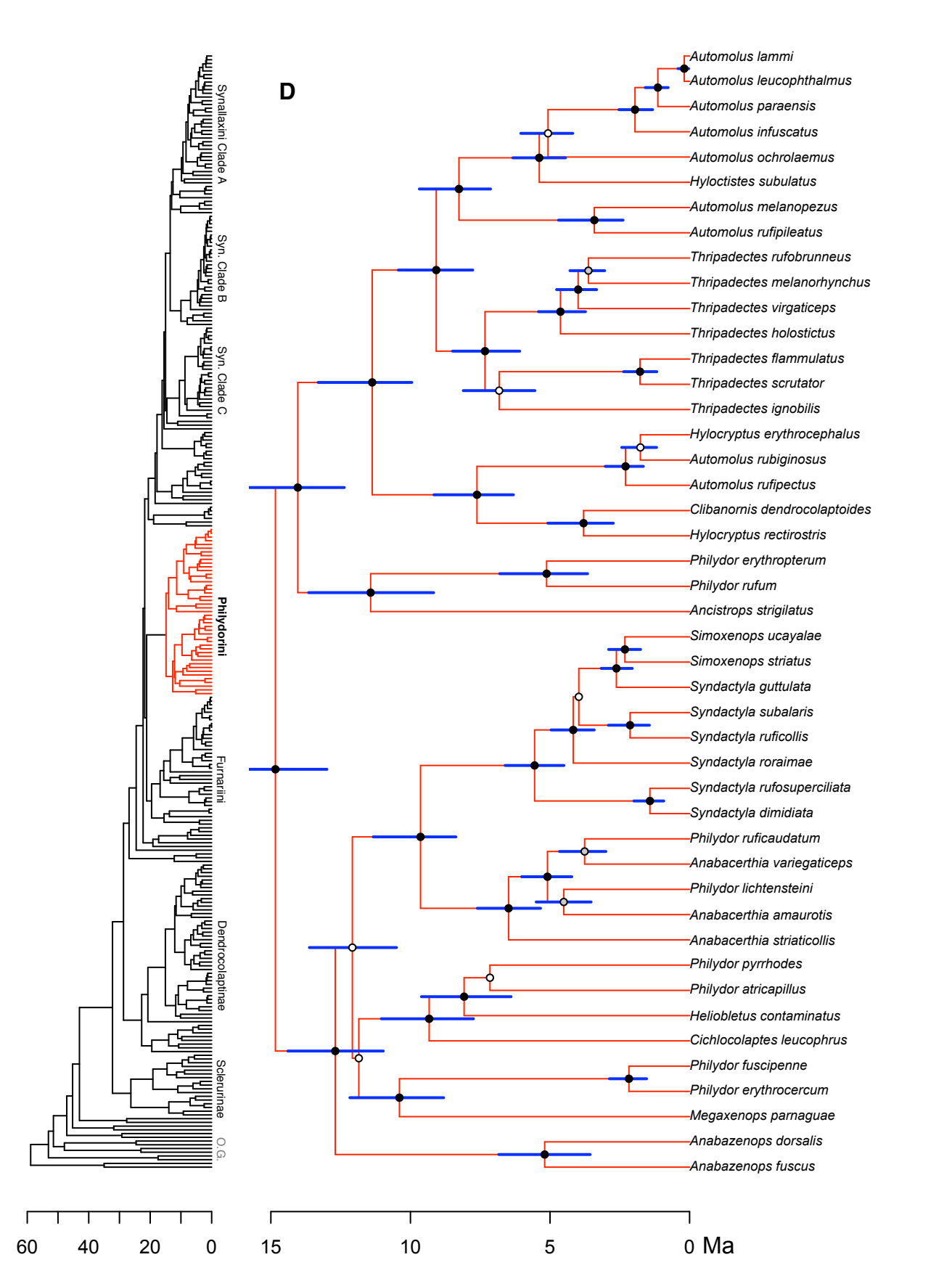
D
Synallaxini Clade A
Syn. Clade B
Syn. Clade C
Philydorini
Furnariini
Dendrocolaptinae
Sclerurinae
O.G.
Automolus lammi
Automolus leucophthalmus
Automolus paraensis
Automolus infuscatus
Automolus ochrolaemus
Hyloctistes subulatus
Automolus melanopezus
Automolus rufipileatus
Thripadectes rufobrunneus
Thripadectes melanorhynchus
Thripadectes virgaticeps
Thripadectes holostictus
Thripadectes flammulatus
Thripadectes scrutator
Thripadectes ignobilis
Hylocryptus erythrocephalus
Automolus rubiginosus
Automolus rufipectus
Clibanornis dendrocolaptoides
Hylocryptus rectirostris
Philydor erythropterum
Philydor rufum
Ancistrops strigilatus
Simoxenops ucayalae
Simoxenops striatus
Syndactyla guttulata
Syndactyla subalaris
Syndactyla ruficollis
Syndactyla roraimae
Syndactyla rufosuperciliata
Syndactyla dimidiata
Philydor ruficaudatum
Anabacerthia variegaticeps
Philydor lichtensteini
Anabacerthia amaurotis
Anabacerthia striaticollis
Philydor pyrrhodes
Philydor atricapillus
Heliobletus contaminatus
Cichlocolaptes leucophrus
Philydor fuscipenne
Philydor erythrocercum
Megaxenops parnaguae
Anabazenops dorsalis
Anabazenops fuscus
60
40
20
0
15
10
5
0 Ma

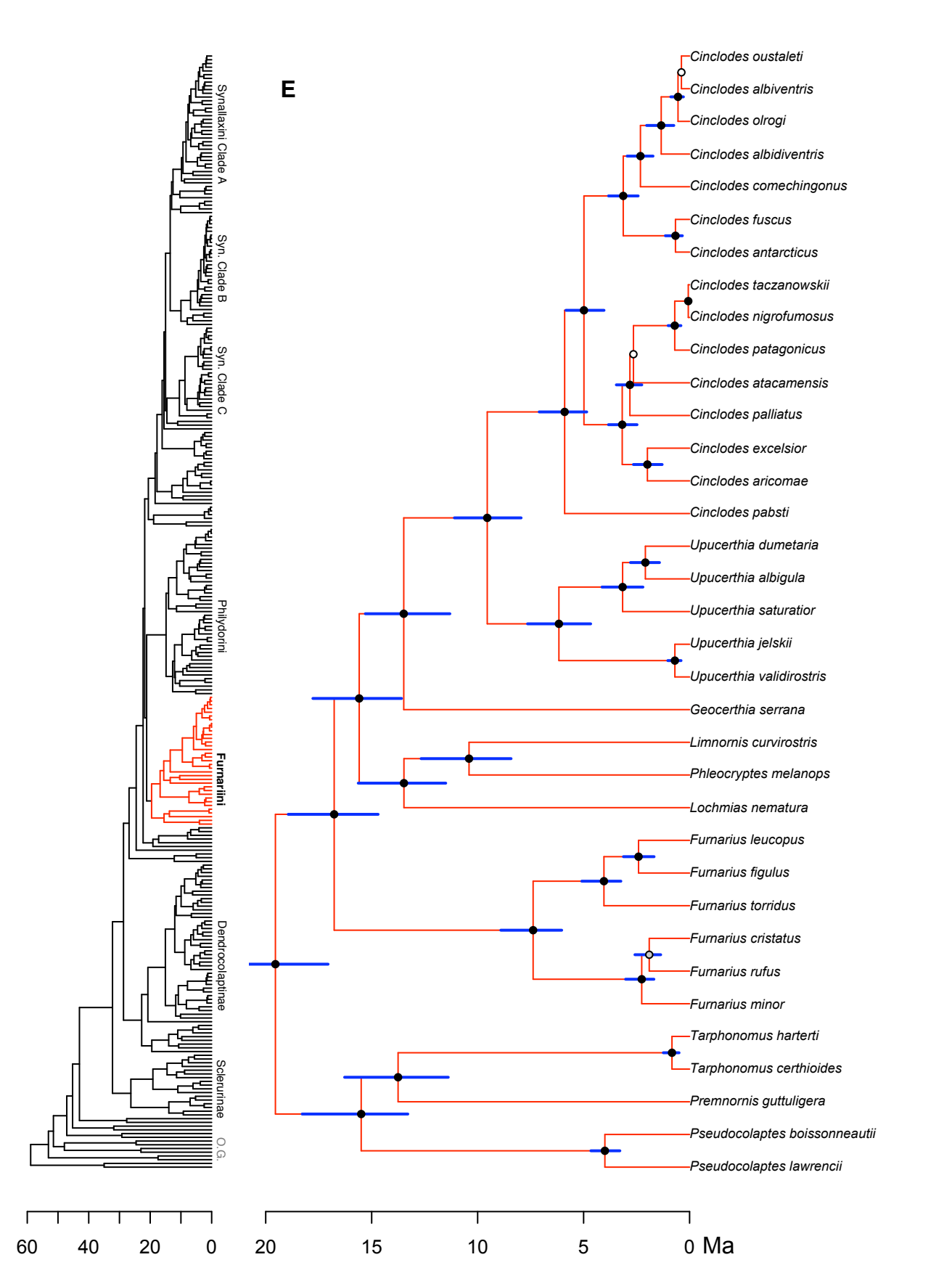
E
Synallaxini Clade A
Syn. Clade B
Syn. Clade C
Philydorini
Furnariini
Dendrocolaptinae
Sclerurinae
O.G.
Cinclodes oustaleti
Cinclodes albiventris
Cinclodes olrogi
Cinclodes albidiventris
Cinclodes comechingonus
Cinclodes fuscus
Cinclodes antarcticus
Cinclodes taczanowskii
Cinclodes nigrofumosus
Cinclodes patagonicus
Cinclodes atacamensis
Cinclodes palliatus
Cinclodes excelsior
Cinclodes aricomae
Cinclodes pabsti
Upucerthia dumetaria
Upucerthia albigula
Upucerthia saturatior
Upucerthia jelskii
Upucerthia validirostris
Geocerthia serrana
Limnornis curvirostris
Phleocryptes melanops
Lochmias nematura
Furnarius leucopus
Furnarius figulus
Furnarius torridus
Furnarius cristatus
Furnarius rufus
Furnarius minor
Tarphonomus harterti
Tarphonomus certhioides
Premnornis guttuligera
Pseudocolaptes boissonneautii
Pseudocolaptes lawrencii
60
40
20
0
20
15
10
5
0 Ma

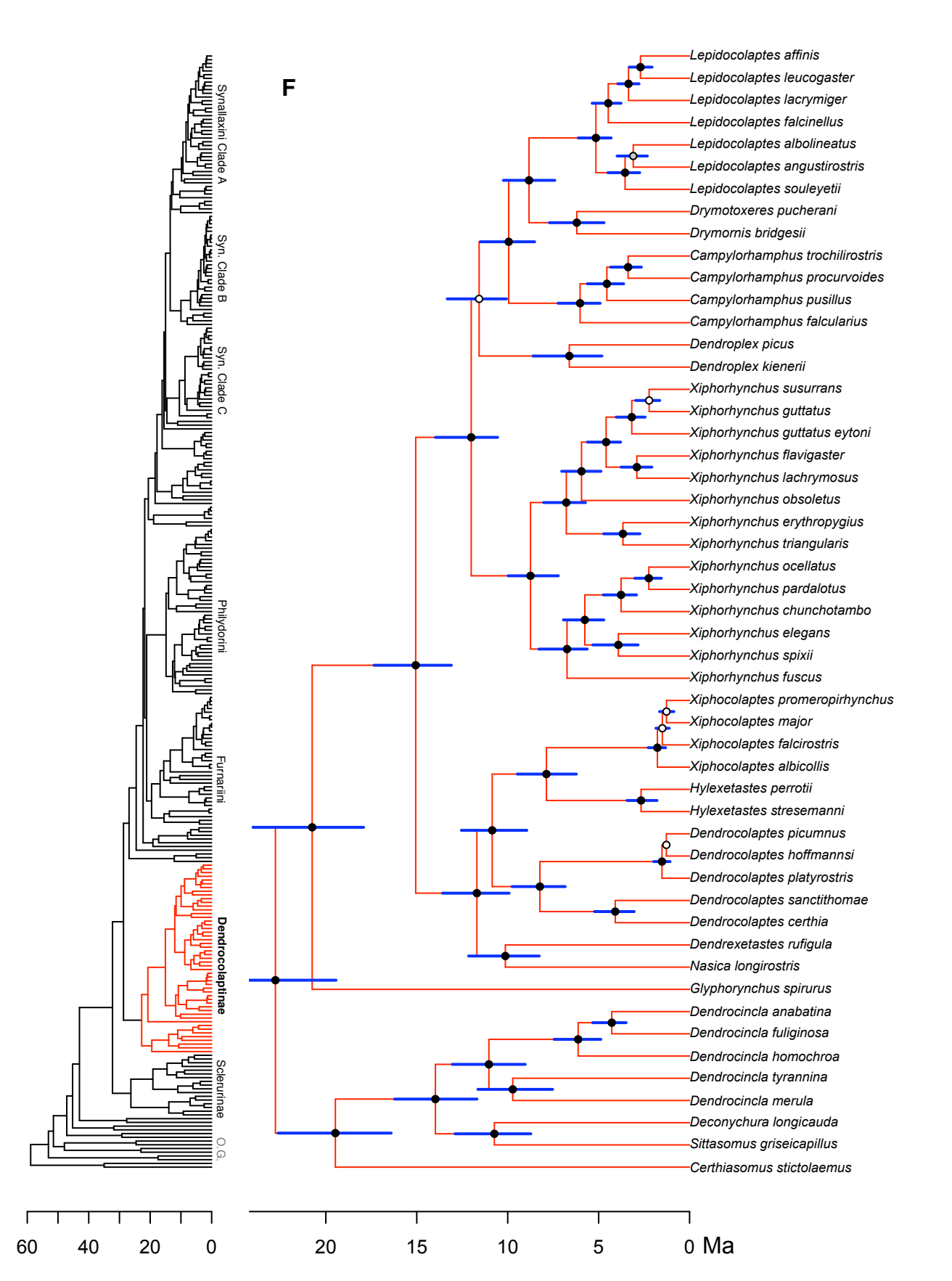
F
Synallaxini Clade A
Syn. Clade B
Syn. Clade C
Philydorini
Furnariini
Dendrocolaptinae
Sclerurinae
O.G.
Lepidocolaptes affinis
Lepidocolaptes leucogaster
Lepidocolaptes lacrymiger
Lepidocolaptes falcinellus
Lepidocolaptes albolineatus
Lepidocolaptes angustirostris
Lepidocolaptes souleyetii
Drymotoxeres pucherani
Drymornis bridgesii
Campylorhamphus trochilirostris
Campylorhamphus procurvoides
Campylorhamphus pusillus
Campylorhamphus falcularius
Dendroplex picus
Dendroplex kienerii
Xiphorhynchus susurrans
Xiphorhynchus guttatus
Xiphorhynchus guttatus eytoni
Xiphorhynchus flavigaster
Xiphorhynchus lachrymosus
Xiphorhynchus obsoletus
Xiphorhynchus erythropygius
Xiphorhynchus triangularis
Xiphorhynchus ocellatus
Xiphorhynchus pardalotus
Xiphorhynchus chunchotambo
Xiphorhynchus elegans
Xiphorhynchus spixii
Xiphorhynchus fuscus
Xiphocolaptes promeropirhynchus
Xiphocolaptes major
Xiphocolaptes falcirostris
Xiphocolaptes albicollis
Hylexetastes perrotii
Hylexetastes stresemanni
Dendrocolaptes picumnus
Dendrocolaptes hoffmannsi
Dendrocolaptes platyrostris
Dendrocolaptes sanctithomae
Dendrocolaptes certhia
Dendrexetastes rufigula
Nasica longirostris
Glyphorynchus spirurus
Dendrocincla anabatina
Dendrocincla fuliginosa
Dendrocincla homochroa
Dendrocincla tyrannina
Dendrocincla merula
Deconychura longicauda
Sittasomus griseicapillus
Certhiasomus stictolaemus
60
40
20
0
20
15
10
5
0 Ma

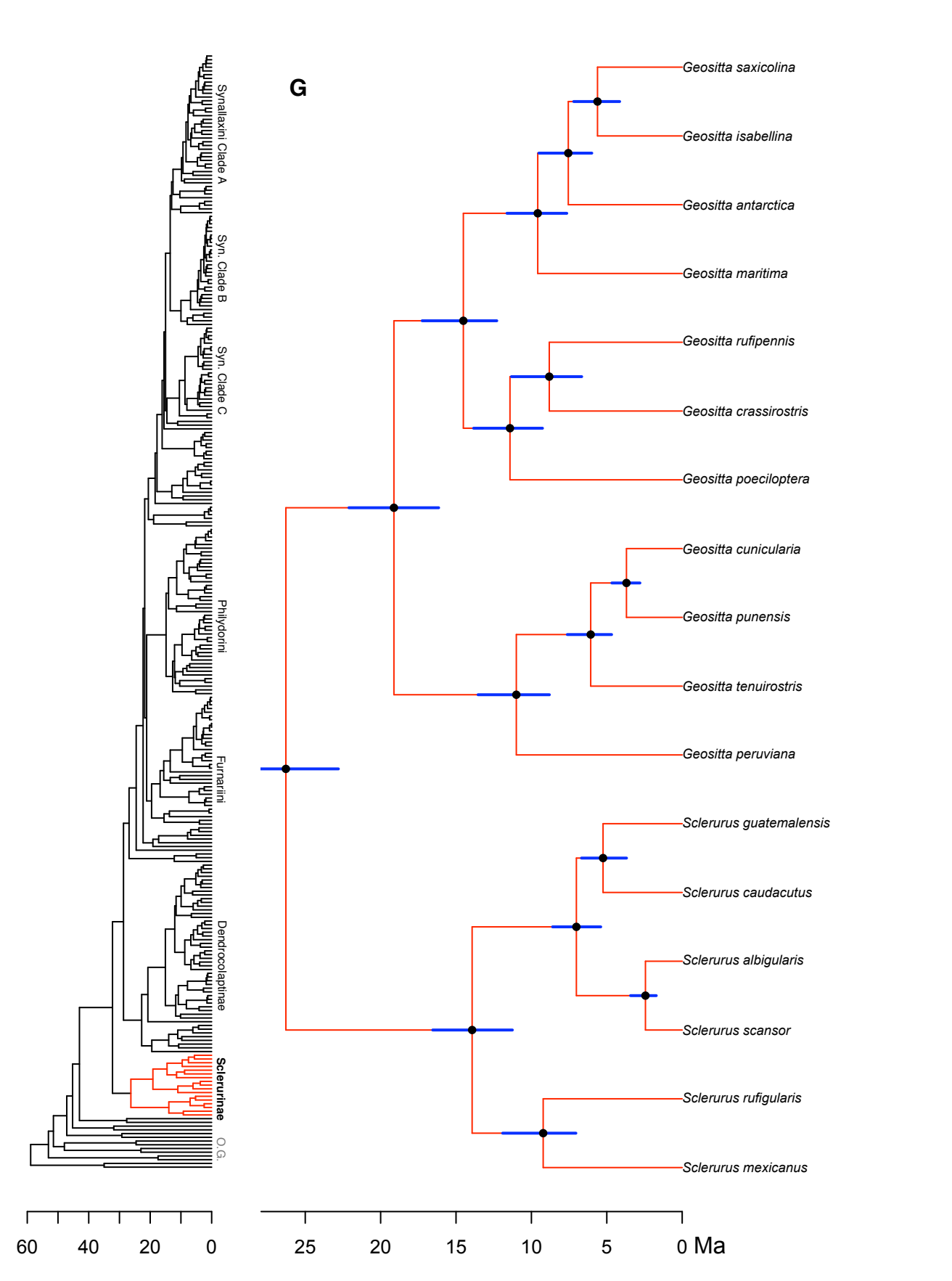
G
Synallaxini Clade A
Syn. Clade B
Syn. Clade C
Philydorini
Furnariini
Dendrocolaptinae
Sclerurinae
O.G.
Geositta saxicolina
Geositta isabellina
Geositta antarctica
Geositta maritima
Geositta rufipennis
Geositta crassirostris
Geositta poeciloptera
Geositta cunicularia
Geositta punensis
Geositta tenuirostris
Geositta peruviana
Sclerurus guatemalensis
Sclerurus caudacutus
Sclerurus albigularis
Sclerurus scansor
Sclerurus rufigularis
Sclerurus mexicanus
60
40
20
0
25
20
15
10
5
0 Ma


H
Synallaxini Clade A
Syn. Clade B
Syn. Clade C
Philydorini
Furnariini
Dendrocolaptinae
Sclerurinae
O.G.
Phacellodomus ruber
Phacellodomus striaticollis
Phacellodomus erythrophthalmus
Phacellodomus dorsalis
Phacellodomus maculipectus
Phacellodomus sibilatrix
Phacellodomus striaticeps
Phacellodomus rufifrons
Synallaxini Clade A
Synallaxini Clade B
Synallaxini Clade C
Hellmayrea gularis
Leptasthenura andicola
Leptasthenura aegithaloides
Leptasthenura fuliginiceps
Leptasthenura striata
Leptasthenura pileata
Leptasthenura striolata
Leptasthenura platensis
Leptasthenura setaria
Leptasthenura xenothorax
Sylviorthorhynchus desmursii
Leptasthenura yanacensis
Aphrastura spinicauda
Margarornis bellulus
Margarornis stellatus
Margarornis squamiger
Margarornis rubiginosus
Premnoplex tatei
Premnoplex brunnescens
Furnariini
Philydorini
Ochetorhynchus phoenicurus
Ochetorhynchus ruficaudus
Ochetorhynchus melanurus
Ochetorhynchus andaecola
Pygarrhichas albogularis
Microxenops milleri
Berlepschia rikeri
Xenops rutilans
Xenops tenuirostris
Xenops minutus
Dendrocolaptinae
Sclerurinae
Chamaeza
Formicarius
Rhinocrypta
Scytalopus
Myrmothera
Grallaria
Pyriglena
Terenura
Pittasoma
Conopophaga
Melanopareia 1
Melanopareia 2
Tyrannus
Tityra
60
40
20
0
60
50
40
30
20
10
0 Ma

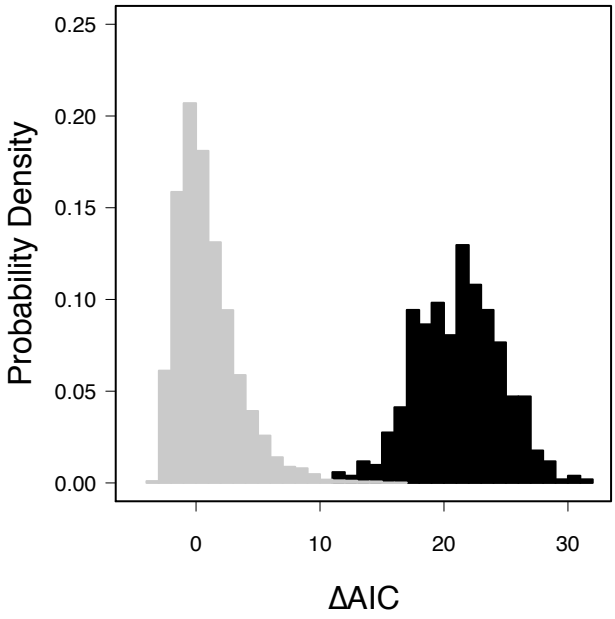
0.25
0.20
0.15
0.10
0.05
0.00
Probability Density
0
10
20
30
ΔAIC

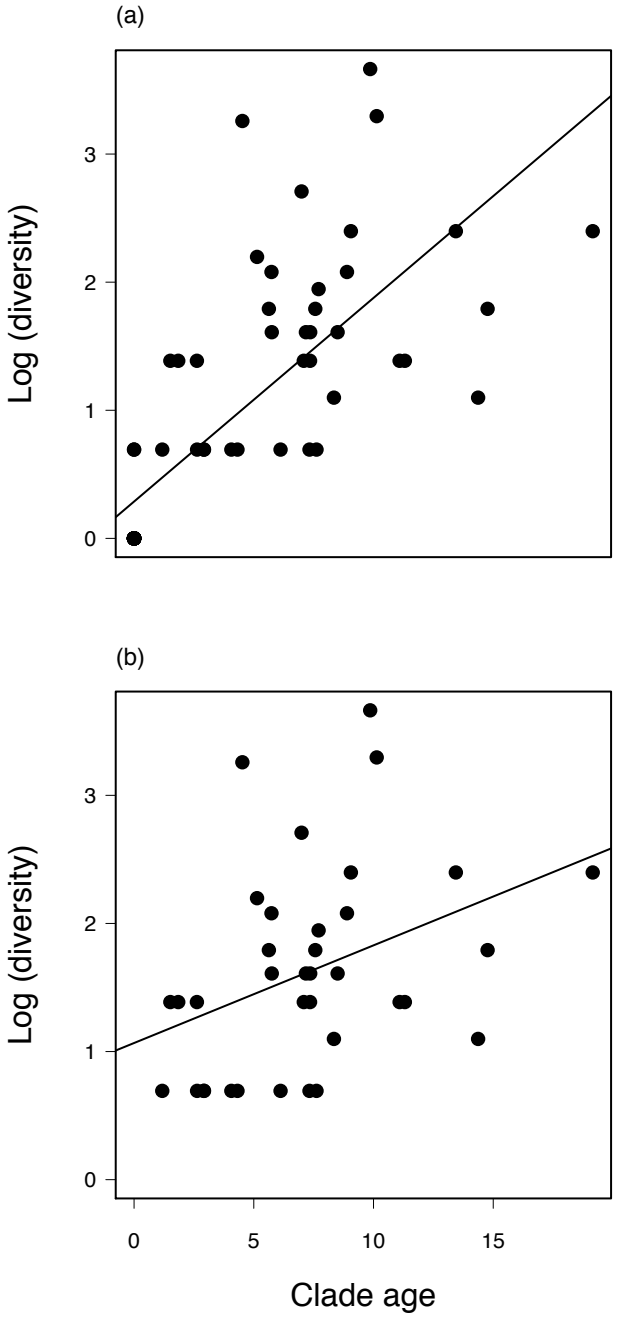
(a)
Log (diversity)
0
1
2
3
(b)
Log (diversity)
0
1
2
3
0
5
10
15
Clade age

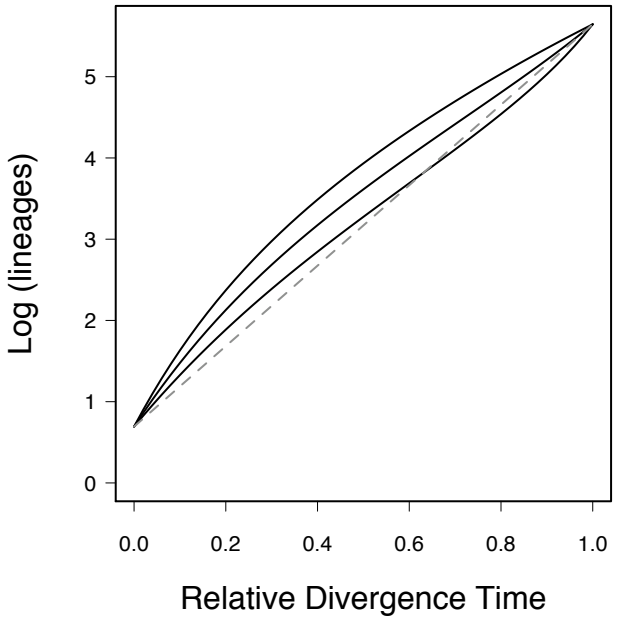
Log (lineages)
0
1
2
3
4
5
0.0
0.2
0.4
0.6
0.8
1.0
Relative Divergence Time

**Table S1: Accession numbers and locality information for samples included in the Furnariidae phylogeny.**

| Taxa | Source | Tissue # | BF7 | COII | ND3 | ND2 | RAGI | RAGII | Locality |
|---|---|---|---|---|---|---|---|---|---|
| *Geositta poeciloptera* | LSUMNS | B13968 | JF974355 | JF974868 | JF974556 | JF975122 | FJ461101 | FJ461003 | BOLIVIA: depto. Santa Cruz; Serranía de Huanchaca, 45km E Florida. |
| *Geositta cunicularia* | LSUMNS | B52013 | JF974356 | JF974869 | JF974557 | JF975123 | | | URUGUAY: depto. Rocha; Camino del Indio, Route 14 km 489. |
| *Geositta tenuirostris* | LSUMNS | B3599 | JF974357 | JF974870 | JF974558 | JF975124 | | | PERU: depto. Huánuco; Huánuco Viejo SE La Unión. |
| *Geositta antarctica* | AMNH | 826117 | JF974358 | JF974871 | AY695032 | AY694992 | | | CHILE: prov. Magallanes; Tierra del Fuego, Estancia Los Tehuelches, ~4 km NE Puerto Nuevo. |
| *Geositta maritima* | LSUMNS | B49692 | JF974359 | JF974872 | JF974559 | JF975125 | | | PERU: depto. Loreto; Lomas de Pachacamac, ~28 km SE Lima. |
| *Geositta peruviana* | LSUMNS | B103811 | JF974360 | JF974873 | AY695037 | JF975126 | | | PERU: depto. Ica; 5 km WNW Pozo Santo. |

| Taxa | Source | Tissue # | BF7 | COII | ND3 | ND2 | RAGI | RAGII | Locality |
|---|---|---|---|---|---|---|---|---|---|
| *Geositta saxicolina* | LSUMNS | B103925 | JF974361 | JF974874 | JF974560 | JF975127 | | | PERU: depto. Lima; ~8 road km NW Chinchan. |
| *Geositta rufipennis* | LSUMNS | B17164 | JF974362 | JF974875 | JF974561 | JF975128 | | | ARGENTINA: prov. Tucumán; Amaicha del Valle, 12 km S, 12 km E. |
| *Geositta isabellina* | AMNH | DOT12181 | EF635308 | EF635333 | EF635352 | AY694995 | FJ461102 | FJ461004 | CHILE: prov. Cordillera; 15 km ENE Embalse El Yeso. |
| *Geositta punensis* | LSUMNS | B103893 | JF974363 | JF974876 | JF974562 | JF975129 | | | PERU: depto. Puno; ~28 Road km S Mazo Cruz. |
| *Geositta crassirostris* | LSUMNS | B103868 | JF974364 | JF974877 | AY695040 | AY695000 | | | PERU: depto. Arequipa; km 54 on Div. Arequipa-Puno Hwy. |
| *Sclerurus mexicanus* | LSUMNS | B35770 | JF974365 | JF974878 | JF974563 | GQ906710 | | | COSTA RICA: prov. Cartago; 11 km SW Pejibaye. |
| *Sclerurus rufigularis* | LSUMNS | B2738 | JF974366 | JF974879 | JF974564 | JF975130 | | | PERU: depto. Loreto; 1 km N Río Napo, 157 km by river NNE Iquitos. |
| *Sclerurus guatemalensis* | LSUMNS | B26538 | JF974367 | JF974880 | JF974565 | JF975131 | | | PANAMA: prov. Colón; 17 km by road NW Gamboa, Río Agua Salud. |

| Taxa | Source | Tissue # | BF7 | COII | ND3 | ND2 | RAGI | RAGII | Locality |
|---|---|---|---|---|---|---|---|---|---|
| *Sclerurus caudacutus* | LSUMNS | B9654 | JF974368 | JF974881 | JF974566 | JF975132 | | | BOLIVIA: depto. Pando; Prov. Nicolás Suárez; ~12 km by road S Cobija, ~8 km W on road to Mucden. |
| *Sclerurus albigularis* | LSUMNS | B5412 | JF974369 | JF974882 | JF974567 | JF975133 | | | PERU: depto. San Martín; 20 km by road NE Tarapoto on road to Yurimaguas. |
| *Sclerurus scansor* | LSUMNS | B25912 | JF974370 | JF974883 | JF974568 | JF975134 | | | PARAGUAY: depto. Caaguazú; Cord. de Caaguazú, 7.5 km E San Carlos. |
| *Ochetorhynchus andaecola* | LSUMNS | B1199 | EF635325 | EF635345 | EF635364 | JF975135 | | | BOLIVIA: depto. La Paz; 2.5 km by road S Mecapaca, ~26 km by road S Calacoto. |
| *Ochetorhynchus ruficaudus* | LSUMNS | B103908 | JF974371 | JF974884 | JF974569 | JF975136 | JF974839 | JF974810 | PERU: depto. Arequipa; km 60 on Div. Arequipa-Julia road, ~10 road km W Chaguata. |
| *Ochetorhynchus phoenicurus* | AMNH | DOT9943 | EF635310 | EF635335 | EF635354 | JF975137 | FJ461105 | FJ461007 | ARGENTINA: prov. Río Negro; 20 km E Norquinco. |

| Taxa | Source | Tissue # | BF7 | COII | ND3 | ND2 | RAGI | RAGII | Locality |
|---|---|---|---|---|---|---|---|---|---|
| *Ochetorhynchus melanura* | AMNH | DOT12148 | JF974372 | JF974885 | JF974570 | JF975138 | FJ461106 | FJ461008 | CHILE: prov. Chacabuco; ~4 km SSW by road from peak of Cerro El Roble. |
| *Upucerthia dumetaria* | AMNH | DOT10396 | JF974373 | JF974886 | JF974571 | JF975139 | FJ461103 | FJ461005 | ARGENTINA: prov. Neuquén; Anelo, Sierra Auca Mahuida. |
| *Upucerthia saturatior* | AMNH | DOT12119 | EF635316 | AY613371 | AY613351 | | | | ARGENTINA: prov. Río Negro; Bariloche, Cerro Perito Moreno, 2 km below Refugio Perito Moreno, ~20 km N El Bolsón. |
| *Upucerthia albigula* | LSUMNS | B61491 | JF974374 | JF974887 | JF974572 | JF975140 | | | PERU: depto. Arequipa; 14 km E Pancarpata. |
| *Upucerthia jelskii* | LSUMNS | B103886 | JF974375 | JF974888 | JF974573 | JF975141 | | | PERU: depto. Tacna; Tacna-Ilave Road, ~25 km NE Tarata. |
| *Upucerthia validirostris* | LSUMNS | B17160 | JF974376 | JF974889 | JF974574 | JF975142 | | | ARGENTINA: prov. Tucumán; Taft de Valle, 12 km N, 4 km W. |
| *Geocerthia serrana* | LSUMNS | B49662 | JF974377 | JF974890 | JF974575 | JF975143 | JF974840 | JF974811 | PERU: depto. Lima; Santa Eulalia road, ~86 km NE Lima. |

| Taxa | Source | Tissue # | BF7 | COII | ND3 | ND2 | RAGI | RAGII | Locality |
|---|---|---|---|---|---|---|---|---|---|
| *Cinclodes excelsior* | LSUMNS | B5935 | JF974378 | AY613378 | AY613358 | JF975144 | | | ECUADOR: prov. Pichincha; W of Papallacta. |
| *Cinclodes aricomae* | FMNH | 391866 | JF974379 | JF974891 | JF974576 | JF975145 | | | PERU: depto. Urubamba; Yanacocha. |
| *Cinclodes fuscus* | AMNH | DOT12169 | EF635312 | AY613380 | AY613360 | JF975146 | | | CHILE: prov. Cordillera; 2 km ENE Embalse El Yeso. |
| *Cinclodes albiventris* | LSUMNS | B22572 | JF974380 | FJ799382 | FJ799435 | | | | BOLIVIA: depto. La Paz; Zongo Valley, 7 km by road N. of Summit. |
| *Cinclodes albidiventris* | LSUMNS | B32706 | JF974381 | FJ799365 | FJ799418 | | | | PERU: depto. Cajamarca; Quebrada Lanchal, ca 8 km ESE Sallique. |
| *Cinclodes comechingonus* | AMNH | DOT12107 | JF974382 | AY613376 | AY613356 | JF975147 | | | ARGENTINA: prov. Córdoba; Punilla, Pampa de Achala, ~7 km E El Condor on Provincial Route 20. |
| *Cinclodes pabsti* | MPEG | 64821 | JF974383 | JF974892 | JF974577 | JF975148 | | | BRAZIL: Rio Grande do Sul; ~36 km NE São José dos Ausentes. |
| *Cinclodes olrogi* | AMNH | DOT12106 | JF974384 | AY613383 | AY613363 | JF975149 | | | ARGENTINA: prov. Córdoba; Punilla, Pampa de Achala, El Condor, Ruta 20. |

| Taxa | Source | Tissue # | BF7 | COII | ND3 | ND2 | RAGI | RAGII | Locality |
|---|---|---|---|---|---|---|---|---|---|
| *Cinclodes oustaleti* | AMNH | DOT12168 | JF974385 | AY613385 | AY613365 | JF975150 | | | CHILE: prov. Cordillera; 2 km ENE Embalse El Yeso. |
| *Cinclodes patagonicus* | LSUMNS | B56831 | JF974386 | JF974893 | JF974578 | JF975151 | | | ARGENTINA: prov. Chubut; ~15 km N Río Pico, Arroyo Negro on Provincial Route 19. |
| *Cinclodes taczanowskii* | LSUMNS | B58461 | JF974387 | JF974894 | JF974579 | JF975152 | | | PERU: depto. Lima; Playa San Antonio, ~13 km SE Chile. |
| *Cinclodes nigrofumosus* | AMNH | DOT12164 | EF635313 | AY613381 | AY613361 | JF975153 | FJ461107 | FJ461009 | CHILE: prov. Petorca; Roca Brava, ~2 km N Zapallar. |
| *Cinclodes antarcticus* | AMNH | 817070 | | AY613373 | AY613353 | | | | CHILE: prov. Magallanes, Isla Gonzalo, Arch. Diego Ramírez,. |
| *Cinclodes atacamensis* | AMNH | DOT12105 | JF974388 | AY613375 | AY613355 | JF975154 | | | ARGENTINA: prov. Córdoba; Punilla, Pampa de Achala, ~8 km E El Cóndor on Provincial Route 20. |
| *Cinclodes palliatus* | LSUMNS | B103923 | JF974389 | AY613387 | AY613367 | JF975155 | | | PERU: depto. Junín; ~14 road km NW |

| Taxa | Source | Tissue # | BF7 | COII | ND3 | ND2 | RAGI | RAGII | Locality |
|---|---|---|---|---|---|---|---|---|---|
| | | | | | | | | | Chinchán on road to Marcapomacocha. |
| *Furnarius figulus* | FMNH | 392828 | EF635314 | EF635337 | EF635355 | JF975156 | | | BRAZIL: Alagoas; Piranhas, Fazenda Bela Vista. |
| *Furnarius leucopus* | FMNH | 433331 | JF974390 | JF974895 | JF974580 | JF975157 | | | PERU: depto. Cuzco; Paucartambo, Consuelo, 15.9 km SW Pilcopata. |
| *Furnarius torridus* | LSUMNS | B4559 | JF974391 | JF974896 | JF974581 | JF975158 | | | PERU: depto. Loreto; island in Río Napo at mouth of Río Yanayacu, ~75 km N Iquitos. |
| *Furnarius minor* | LSUMNS | B42939 | JF974392 | JF974897 | JF974582 | JF975159 | | | PERU: depto. Loreto; River island in Río Marañón at mouth of Río Morona. |
| *Furnarius rufus* | AMNH | DOT10431 | GQ906726 | GQ906740 | GQ922581 | GQ906711 | AY056995 | AY443149 | ARGENTINA: prov. Neuquén; Confluencia, Centenario. |
| *Furnarius cristatus* | LSUMNS | B26022 | JF974393 | JF974898 | JF974583 | JF975160 | | | PARAGUAY: depto. Presidente Hayes; Estancia Zalazar. |
| *Limnornis curvirostris* | LSUMNS | B52024 | JF974394 | JF974899 | JF974584 | JF975161 | JF974841 | JF974812 | URUGUAY: depto. Colonia; Conchillas, Arenera de Puerto |

| Taxa | Source | Tissue # | BF7 | COII | ND3 | ND2 | RAGI | RAGII | Locality |
|---|---|---|---|---|---|---|---|---|---|
| | | | | | | | | | Conchillas. |
| *Limnoctites rectirostris* | AMNH | DOT12093 | JF974395 | JF974900 | JF974585 | JF975162 | FJ461108 | FJ461010 | ARGENTINA: prov. Buenos Aires; Partido Escobar, 15 km N Belén de Escobar. |
| *Phleocryptes melanops* | AMNH | DOT9917 | JF974396 | JF974901 | JF974586 | JF975163 | FJ461109 | FJ461011 | ARGENTINA: prov. Buenos Aires; Partido Escobar. |
| *Aphrastura spinicauda* | AMNH | DOT12110 | JF974397 | JF974902 | JF974587 | JF975164 | FJ461110 | FJ461012 | ARGENTINA: prov. Río Negro; Bariloche, Cerro Perito Moreno, ~20 km N El Bolsón. |
| *Leptasthenura fuliginiceps* | FMNH | 334444 | JF974398 | JF974903 | JF974588 | JF975165 | | | BOLIVIA: depto. Cochabamba; Cochabamba-Oruro Rd, km 31. |
| *Leptasthenura yanacensis* | FMNH | 391876 | JF974399 | JF974904 | JF974589 | JF975166 | | | PERU: depto. Lima; Quichas. |
| *Leptasthenura platensis* | USNM | 13608 | JF974400 | JF974905 | JF974590 | JF975167 | | | URUGUAY: depto. Soriano; Cardona, 16 km ENE, at Arroyo Grande. |
| *Leptasthenura* | AMNH | DOT10306 | JF974401 | JF974906 | JF974591 | JF975168 | FJ461111 | FJ461013 | ARGENTINA: prov. Neuquén; Anelo, |

| Taxa | Source | Tissue # | BF7 | COII | ND3 | ND2 | RAGI | RAGII | Locality |
|---|---|---|---|---|---|---|---|---|---|
| *aegithaloides* | | | | | | | | | Sierra Auca Mahuida. |
| *Leptasthenura striolata* | MCN | 2810 | JF974402 | JF974907 | JF974592 | JF975169 | | | BRAZIL: Rio Grande do Sul; São Francisco de Paula. |
| *Leptasthenura pileata* | LSUMNS | B3584 | JF974403 | JF974908 | JF974593 | JF975170 | | | PERU: depto. Huánuco; Nuevas Flores (Cullquish) on Río Marañón. |
| *Leptasthenura xenothorax* | FMNH | 391868 | JF974404 | JF974909 | JF974594 | JF975171 | | | PERU: depto. Cuzco; Yanacocha. |
| *Leptasthenura striata* | LSUMNS | B103880 | JF974405 | JF974910 | JF974595 | JF975172 | | | PERU: depto. Tacna; Tacna-Ilave Road, ~25 km NE Tarata. |
| *Leptasthenura andicola* | LSUMNS | B103831 | JF974406 | JF974911 | JF974596 | JF975173 | | | PERU: depto. Ayacucho; Pampa Galeras, 25km WNW on Puquio. |
| *Leptasthenura setaria* | MPEG | 64824 | JF974407 | JF974912 | JF974597 | JF975174 | | | BRAZIL: Rio Grande do Sul, Fazenda Monte Negro, ~30km NE São José dos Ausentes. |
| *Spartonoica maluroides* | AMNH | DOT12089 | JF974408 | JF974913 | JF974598 | JF975175 | FJ461112 | FJ461014 | ARGENTINA: prov. Buenos Aires; Partido de General Lavalle, Cabo San |

| Taxa | Source | Tissue # | BF7 | COII | ND3 | ND2 | RAGI | RAGII | Locality |
|---|---|---|---|---|---|---|---|---|---|
| | | | | | | | | | Antonio, Reserva Punta Rasal. |
| *Sylviorthorhynchus desmursii* | AMNH | DOT12209 | JF974409 | JF974914 | JF974599 | JF975176 | FJ461113 | FJ461015 | CHILE: prov. Malleco; ~12 km by road S Icalma. |
| *Schizoeaca perijana* | ICN | AMC879 | JF974410 | JF974915 | JF974600 | JF975177 | | | COLOMBIA: depto. Cesar, Mun. Manaure, Sabana Rubia. |
| *Schizoeaca coryi* | COP | AMC1238 | | JF974916 | JF974601 | JF975178 | | | VENEZUELA: edo. Táchira, PN Páramos El Batallón y La Negra, Sector La Barrosa. |
| *Schizoeaca fuliginosa* | LSUMNS | B30039 | JF974411 | JF974917 | JF974602 | JF975179 | | | ECUADOR: prov. Carchi; ~8 km W Tufino. |
| *Schizoeaca griseomurina* | LSUMNS | B34804 | JF974412 | JF974918 | JF974603 | JF975180 | | | PERU: depto. Cajamarca; Cordillera del Cóndor; Picorana. |
| *Schizoeaca palpebralis* | LSUMNS | B49625 | JF974413 | JF974919 | JF974604 | JF975181 | | | PERU: depto. Junín; E Comas, ~45 km NE Huancayo. |
| *Schizoeaca vilcabambae* | FMNH | 390681 | JF974414 | JF974920 | JF974605 | JF975182 | | | PERU: depto. Junín; Cordillera Vilcabamba, headwaters Río Pomureni. |

| Taxa | Source | Tissue # | BF7 | COII | ND3 | ND2 | RAGI | RAGII | Locality |
|---|---|---|---|---|---|---|---|---|---|
| *Schizoeaca helleri* | AMNH | DOT2479 | JF974415 | JF974921 | JF974606 | JF975183 | FJ461114 | FJ461016 | BOLIVIA: depto. La Paz; Tojoloque, near Queara. |
| *Schizoeaca harterti* | LSUMNS | B1271 | JF974416 | JF974922 | JF974607 | JF975184 | | | BOLIVIA: depto. La Paz; ~1km S Chuspipata. |
| *Oreophylax moreirae* | UFMGDZ | 3282 | JF974417 | JF974923 | JF974608 | JF975185 | JF974842 | JF974813 | BRAZIL: Minas Gerais; Pico do Inficionado, Serra do Caraça, Mun. de Catas Altas. |
| *Schoeniophylax phryganophilus* | FMNH | 334448 | | JF974924 | JF974609 | JF975186 | FJ461115 | FJ461017 | BOLIVIA: depto. Beni; Trinidad. |
| *Synallaxis ruficapilla* | LSUMNS | B25955 | | JF974925 | JF974610 | JF975187 | | | PARAGUAY: depto. Caazapá; Cor. de Caaguazú, 7.5 km E. San Carlos. |
| *Synallaxis cinerascens* | AMNH | DOT12077 | | AY489495 | AY489543 | JF975188 | | | ARGENTINA: prov. Misiones; Parque Provincal Urugua-I, ~1 km W park headquarters, Ruta Provincial 19. |
| *Synallaxis subpudica* | Andes-O | 355 | | JF974926 | JF974611 | JF975189 | | | COLOMBIA: depto. Cundinamarca; La Calera, El Hato, Finca La Valquiria. |

| Taxa | Source | Tissue # | BF7 | COII | ND3 | ND2 | RAGI | RAGII | Locality |
|---|---|---|---|---|---|---|---|---|---|
| *Synallaxis frontalis* | LSUMNS | B25806 | | JF974927 | JF974612 | JF975190 | | | BOLIVIA: depto. Santa Cruz; Chuchial, ~37 km SW Samaipata. |
| *Synallaxis azarae* | LSUMNS | B1232 | | JF974928 | JF974613 | JF975191 | | | BOLIVIA: depto. La Paz; ~1km S Chuspipata. |
| *Synallaxis courseni* | LSUMNS | B19225 | | JF974929 | JF974614 | JF975192 | | | PERU: depto. Apurímac; Cerro, Turronmucco Nevado Ampay. |
| *Synallaxis albescens* | AMNH | DOT2295 | | JF974930 | JF974615 | JF975193 | FJ461118 | FJ461020 | BOLIVIA: depto. Santa Cruz; Prov. Velasco; near localidad El Tun, 300 m N of Río Mercedes. |
| *Synallaxis albigularis* | LSUMNS | B44453 | | JF974931 | JF974616 | JF975194 | | | PERU: depto. Loreto; Isla Pasto; Río Amazonas opposite Aysana, ~80 km NE Iquitos. |
| *Synallaxis spixi* | LSUMNS | B25984 | | JF974932 | JF974617 | JF975195 | | | PARAGUAY: depto. Caazapá; Cor. de Caaguazú, 7.5 km E. San Carlos. |
| *Synallaxis hypospodia* | KU | B3122 | | JF974933 | JF974618 | JF975196 | | | PARAGUAY: Alto Paraguay; Río Negro, W bank 8 km above mouth. |

| Taxa | Source | Tissue # | BF7 | COII | ND3 | ND2 | RAGI | RAGII | Locality |
|---|---|---|---|---|---|---|---|---|---|
| *Synallaxis rutilans* | LSUMNS | B42924 | | JF974934 | JF974619 | HM449849 | | | PERU: depto. Loreto; ~54 km NNW mouth of Río Morona, on west bank. |
| *Synallaxis cherriei* | LSUMNS | B46221 | | JF974935 | JF974620 | JF975197 | | | PERU: depto. San Martin; Quebrada Upaquilia ~26 km SSE Tarajato. |
| *Synallaxis unirufa* | LSUMNS | B6226 | | JF974936 | JF974621 | JF975198 | | | ECUADOR: prov. Morona-Santiago; W slope Cordillera del Cutucú, S trail from Logroño to Yaupi. |
| *Synallaxis castanea* | AMNH | DOT5051 | | JF974937 | JF974622 | JF975199 | | | VENEZUELA: edo. Aragua; km 40 on El Junquito/Col. Tovar Rd. |
| *Synallaxis erythrothorax* | LSUMNS | B60803 | | JF974938 | JF974623 | JF975200 | | | HONDURAS: depto. Atlantida; Lancetilla Botanical Garden entrance road. |
| *Synallaxis brachyura* | LSUMNS | B12071 | | JF974939 | JF974624 | JF975201 | | | ECUADOR: prov. Pichincha; Mindo. |
| *Synallaxis tithys* | ANSP | 18507 | | JF974940 | JF974625 | JF975202 | | | ECUADOR: prov. Manabí; Cerro San Sebastian, Machililla NP. |
| *Synallaxis propinqua* | LSUMNS | B43083 | | JF974941 | JF974626 | JF975203 | JF974843 | JF974814 | PERU: depto. Loreto; river island in Río |

| Taxa | Source | Tissue # | BF7 | COII | ND3 | ND2 | RAGI | RAGII | Locality |
|---|---|---|---|---|---|---|---|---|---|
| | | | | | | | | | Marañón at mouth of Río Morona. |
| *Synallaxis macconnelli* | LSUMNS | B55261 | | JF974942 | JF974627 | JF975204 | | | SURINAME: Sipaliwini; Balchuis Gebergte, ~78 km S Apura on Nickene River. |
| *Synallaxis moesta* | LSUMNS | B44663 | | JF974943 | JF974628 | JF975205 | | | PERU: depto. San Martín; ~33 km NE Florida. |
| *Synallaxis cabanisi* | LSUMNS | B2013 | | JF974944 | JF974629 | HM449848 | | | PERU: depto. Pasco; Km 41 on Villa Rica - Puerto Bermudez highway. |
| *Synallaxis maranonica* | LSUMNS | B32940 | | JF974945 | JF974630 | JF975206 | | | PERU: depto. Cajamarca; Las Juntas, junction of Ríos Tabaconas and Chinchipe. |
| *Synallaxis gujanensis* | LSUMNS | B55226 | | JF974946 | JF974631 | JF975207 | | | SURINAME: Sipaliwini; Balchuis Gebergte, ~78 km S Apura on Nickene River. |
| *Synallaxis albilora* | LSUMNS | B37894 | | JF974947 | JF974632 | JF975208 | | | BOLIVIA: depto. Santa Cruz; Santa Fe: ~138km SW San Matías. |

| Taxa | Source | Tissue # | BF7 | COII | ND3 | ND2 | RAGI | RAGII | Locality |
|---|---|---|---|---|---|---|---|---|---|
| *Synallaxis scutata* | LSUMNS | B37934 | | JF974948 | JF974633 | JF975209 | FJ461117 | FJ461019 | BOLIVIA: depto. Santa Cruz; Santa Fe: ~138km SW San Matías. |
| *Synallaxis candei* | COP | ML800 | | JF974949 | JF974634 | HM125608 | | | VENEZUELA: edo. Zulia; Hacienda Grano de Oro. |
| *Synallaxis kollari* | USNM | B19395 | | JF974950 | JF974635 | JF975210 | | | GUYANA: region Upper Takutu-Upper Essequibo; Karasabai, ca 17 km SSW at Ireng River. |
| *Synallaxis cinnamomea* | COP | JP237 | | HM125635 | JF974636 | HM125604 | | | VENEZUELA: edo. Sucre; Parque Nacional Península de Paria. Sector Las Melenas. |
| *Synallaxis zimmeri* | LSUMNS | B44781 | | JF974951 | JF974637 | JF975211 | | | PERU: depto. La Libertad, 4 km ESE Sinsicap (ca. 60 km E Trujillo), 2090m. |
| *Synallaxis stictothorax* | LSUMNS | B5197 | | JF974952 | JF974638 | JF975212 | FJ461116 | FJ461018 | PERU: depto. Lambayeque; Las Pampas; km 885 Pan-American Hwy, 11 km from Olmos. |
| *Siptornopsis* | LSUMNS | B49709 | | JF974953 | JF974639 | JF975213 | JF974844 | JF974815 | PERU: depto. Cajamarca; ~23 km NNW |

| Taxa | Source | Tissue # | BF7 | COII | ND3 | ND2 | RAGI | RAGII | Locality |
|---|---|---|---|---|---|---|---|---|---|
| *hypochondriaca* | | | | | | | | | Cajamarca. |
| *Gyalophylax hellmayri* | FMNH | 392475 | | JF974954 | JF974640 | JF975214 | FJ461119 | FJ461021 | BRAZIL: Pernambuco. |
| *Hellmayrea gularis* | LSUMNS | B32238 | JF974418 | JF974955 | JF974641 | JF975215 | FJ461120 | FJ461022 | PERU: depto. Cajamarca; Quebrada Lanchal ~ 8 km ESE Sallique. |
| *Cranioleuca marcapatae* | FMNH | 390677 | | JF974956 | JF974642 | JF975216 | | | PERU: depto. Junín; Cordillera Vilcabamba, headwaters Río Pomureni. |
| *Cranioleuca albiceps* | LSUMNS | B1231 | | JF974957 | JF974643 | JF975217 | | | BOLIVIA: depto. La Paz; ~1km S Chuspipata. |
| *Cranioleuca vulpina* | LSUMNS | B25425 | | JF974958 | JF974644 | JF975218 | | | BRAZIL: Amazonas; Rio Solimões, Ilha Marchantaria, ~15 km S Manaus. |
| *Cranioleuca vulpecula* | LSUMNS | B3181 | | JF974959 | JF974645 | JF975219 | | | PERU: depto. Loreto; Isla Ronsoco, Río Napo opposite Libertad, 80 km N Iquitos. |
| *Cranioleuca sulphurifera* | LSUMNS | B52009 | | JF974960 | JF974646 | JF975220 | JF974845 | JF974816 | URUGUAY: depto. Colonia; Conchillas, Arenera de Puerto Conchillas. |

| Taxa | Source | Tissue # | BF7 | COII | ND3 | ND2 | RAGI | RAGII | Locality |
|---|---|---|---|---|---|---|---|---|---|
| *Cranioleuca subcristata* | COP | IC1064 | | JF974961 | JF974647 | HM125611 | | | VENEZUELA: Barinas; Calderas. |
| *Cranioleuca pyrrhophia* | LSUMNS | B52007 | | JF974962 | JF974648 | JF975221 | | | URUGUAY: depto. Cerro Largo; Sierra de los Ríos, Arroyo Sarandí, Paso Real. |
| *Cranioleuca obsoleta* | MPEG | 64815 | | JF974963 | JF974649 | JF975222 | | | BRAZIL: Rio Grande do Sul; Fazenda Monte Negro, ~30km NE São José dos Ausentes. |
| *Cranioleuca pallida* | FMNH | 395422 | | JF974964 | JF974650 | JF975223 | | | BRAZIL: São Paulo; Boracéia. |
| *Cranioleuca semicinerea* | FMNH | 399207 | | JF974965 | JF974651 | JF975224 | | | BRAZIL: Pernambuco; Taquaritinga. |
| *Cranioleuca albicapilla* | LSUMNS | B49667 | | JF974966 | JF974652 | JF975225 | | | PERU: depto. Junín; Lampa, ~39 km ENE Huancayo. |
| *Cranioleuca erythrops* | LSUMNS | B1364 | | JF974967 | JF974653 | JF975226 | FJ461121 | FJ461023 | PANAMA: prov. Darién; ~9 km NW Cana on slopes Cerro Pirre. |
| *Cranioleuca demissa* | LSUMNS | B48507 | | JF974968 | JF974654 | JF975227 | | | GUYANA: S slope Kopinang Mountain, ~ 9 km W Kopinang. |
| *Cranioleuca hellmayri* | Andes-O | 328 | | JF974969 | JF974655 | JF975228 | | | COLOMBIA: depto. Magdalena; Sierra |

| Taxa | Source | Tissue # | BF7 | COII | ND3 | ND2 | RAGI | RAGII | Locality |
|---|---|---|---|---|---|---|---|---|---|
| | | | | | | | | | Nevada de Santa Marta, Cerro San Lorenzo, Hacienda Cincinnati. |
| *Cranioleuca curtata* | LSUMNS | B44590 | | JF974970 | JF974656 | JF975229 | | | PERU: depto. San Martín; ~24 km ENE Florida. |
| *Cranioleuca antisiensis* | LSUMNS | B31684 | | JF974971 | JF974657 | JF975230 | | | PERU: depto. Cajamarca; El Espino. |
| *Cranioleuca baroni* | LSUMNS | B3597 | | JF974972 | JF974658 | JF975231 | | | PERU: depto. Huánuco; Quebrada Huanuash, 4 km by road NW Nuevas Flores (Cullquish). |
| *Cranioleuca gutturata* | LSUMNS | B4819 | | JF974973 | JF974659 | JF975232 | JF974846 | JF974817 | PERU: depto. Loreto; S Río Amazonas, ~10 km SSW mouth Río Napo on E bank Quebrada Vainilla. |
| *Cranioleuca muelleri* | LSUMNS | B25422 | | JF974974 | JF974660 | JF975233 | | | BRAZIL: Amazonas; Rio Solimões, Ilha Marchantaria, ~15 km S Manaus. |
| *Certhiaxis cinnamomeus* | AMNH | DOT6190 | | JF974975 | JF974661 | JF975234 | FJ461122 | FJ461024 | BOLIVIA: depto. Santa Cruz; Prov. Velasco; near localidad El Tun, 300 m N of Río Mercedes. |

| Taxa | Source | Tissue # | BF7 | COII | ND3 | ND2 | RAGI | RAGII | Locality |
|---|---|---|---|---|---|---|---|---|---|
| *Certhiaxis mustelinus* | LSUMNS | B45889 | | JF974976 | JF974662 | JF975235 | | | BRAZIL: Amazonas; Manaus, Bairro Eldorado. |
| *Thripophaga cherriei* | COP | ML983 | | JF974977 | JF974663 | JF975236 | JF974847 | JF974818 | VENEZUELA: Amazonas; Capuana, Río Orinoco. |
| *Thripophaga fusciceps* | LSUMNS | B7607 | | JF974978 | JF974664 | JF975237 | FJ461123 | FJ461025 | BOLIVIA: depto. Beni; Cercado; 6 km by rd. SE Trinidad. |
| *Thripophaga berlepschi* | LSUMNS | B61293 | | JF974979 | JF974665 | JF975238 | JF974848 | JF974819 | PERU: depto. Amazonas; 5 km SE Leimebamba. |
| *Asthenes pudibunda* | LSUMNS | B103915 | JF974419 | JF974980 | JF974666 | JF975239 | JF974849 | JF974820 | PERU: depto. Ayacucho; km 48 on Nazca-Puquio Road. |
| *Asthenes ottonis* | LSUMNS | B61395 | JF974420 | JF974981 | JF974667 | JF975240 | | | PERU: depto. Cusco; 1 km E Huacarpay. |
| *Asthenes modesta* | LSUMNS | B103883 | JF974421 | JF974982 | JF974668 | JF975241 | | | PERU: depto. Tacna; Tacna-Ilave Road, ~25 km NE Tarata. |
| *Pseudasthenes cactorum* | LSUMNS | B103812 | JF974422 | JF974983 | JF974669 | JF975242 | JF974850 | JF974821 | PERU: depto. Ica; 24 km on Nazca-Purquio Road. |

| Taxa | Source | Tissue # | BF7 | COII | ND3 | ND2 | RAGI | RAGII | Locality |
|---|---|---|---|---|---|---|---|---|---|
| *Asthenes humilis* | FMNH | F391862 | JF974423 | JF974984 | JF974670 | JF975243 | FJ461126 | FJ461028 | PERU: depto. Lima; Maticuna. |
| *Asthenes wyatti* | LSUMNS | B103905 | JF974424 | JF974985 | JF974671 | JF975244 | | | PERU: depto. Puno. |
| *Asthenes sclateri* | AMNH | DOT12103 | JF974425 | JF974986 | JF974672 | JF975245 | | | ARGENTINA: prov. Córdoba; Punilla, Pampa de Achala, ~ 8 km E El Cóndor on Provincial Route 20. |
| *Asthenes anthoides* | LSUMNS | B56816 | JF974426 | JF974987 | JF974673 | JF975246 | | | ARGENTINA: prov. Chubut; 16 km WNW Río Pico, Estancia Tres Valles on Provincial Route 19. |
| *Asthenes hudsoni* | USNM | B6349 | JF974427 | JF974988 | JF974674 | JF975247 | | | URUGUAY: depto. Soriano; Cardona, ca 9 km N, at Estancia Santa Emilia. |
| *Asthenes urubambensis* | LSUMNS | B8311 | JF974428 | JF974989 | JF974675 | JF975248 | FJ461124 | FJ461026 | PERU: depto. Pasco; Millpo, E Tambo de Vacas on Pozuzo-Chaglla trail. |
| *Asthenes flammulata* | LSUMNS | B32093 | JF974429 | JF974990 | JF974676 | JF975249 | | | PERU: depto. Cajamarca; Quebrada Lanchal ~8 km ESE Sallique. |
| *Asthenes virgata* | LSUMNS | B61350 | JF974430 | JF974991 | JF974677 | JF975250 | | | PERU: depto. Junín; 2 km N Casapalca. |

| Taxa | Source | Tissue # | BF7 | COII | ND3 | ND2 | RAGI | RAGII | Locality |
|---|---|---|---|---|---|---|---|---|---|
| *Asthenes maculicauda* | AMNH | DOT2484 | JF974431 | JF974992 | JF974678 | JF975251 | | | BOLIVIA: depto. La Paz; Franz Tamayo, Tojoloque, near Queara. |
| *Asthenes pyrrholeuca* | LSUMNS | B56783 | JF974432 | JF974993 | JF974679 | JF975252 | | | ARGENTINA: prov. Chubut; 22 km N Puerto Madryn on Provincial Route 1. |
| *Pseudasthenes humicola* | AMNH | DOT12194 | JF974433 | JF974994 | JF974680 | JF975253 | | | CHILE: prov. Chacabuco; Colina, El Potezuelo. |
| *Asthenes dorbignyi* | LSUMNS | B95386 | JF974434 | JF974995 | JF974681 | | | | BOLIVIA: depto. La Paz; Huajchilla, 18 rd km S Calacoto. |
| *Pseudasthenes steinbachi* | AMNH | DOT10390 | JF974435 | JF974996 | JF974682 | JF975254 | | | ARGENTINA: prov. Neuquén; Anelo, Sierra Auca Mahuida. |
| *Asthenes baeri* | AMNH | DOT12134 | JF974436 | JF974997 | JF974683 | JF975255 | FJ461125 | FJ461027 | ARGENTINA: prov. Buenos Aires; Partido Patagones, ~35 km E Cármen de Patagones, on National Route 3. |
| *Asthenes luizae* | UFMG | B3066 | JF974437 | JF974998 | JF974684 | JF975256 | | | BRAZIL: Minas Gerais; Cardeal Mota, Serra do Cipó. |
| *Pseudasthenes* | LSUMNS | B56798 | JF974438 | JF974999 | JF974685 | JF975257 | | | ARGENTINA: prov. Chubut; ~75 km |

| Taxa | Source | Tissue # | BF7 | COII | ND3 | ND2 | RAGI | RAGII | Locality |
|---|---|---|---|---|---|---|---|---|---|
| *patagonica* | | | | | | | | | W Puerto Madryn, Estancia Sierra Colorada on Provincial Route 8. |
| *Phacellodomus rufifrons* | AMNH | DOT2305 | JF974439 | JF975000 | JF974686 | JF975258 | FJ461127 | FJ461029 | BOLIVIA: depto. Santa Cruz; Prov. Velasco; near localidad El Tun, 300 m N of Río Mercedes. |
| *Phacellodomus sibilatrix* | LSUMNS | B19109 | JF974440 | JF975001 | JF974687 | JF975259 | | | BOLIVIA: depto. Santa Cruz; Cordillera; Estancia Perforación, ~130 km E Charagua. |
| *Phacellodomus striaticeps* | LSUMNS | B106732 | JF974441 | JF975002 | JF974688 | JF975260 | | | BOLIVIA: depto. Cochabamba. |
| *Phacellodomus maculipectus* | KU | 9737 | JF974442 | JF975003 | JF974689 | JF975261 | | | ARGENTINA: prov. Jujuy; E slope Sierra Santa Barbara. |
| *Phacellodomus striaticollis* | CUMV | 50657 | JF974443 | JF975004 | JF974690 | JF975262 | | | URUGUAY: depto. Cerro Largo; Río Yaguarón. |
| *Phacellodomus dorsalis* | LSUMNS | B49701 | JF974444 | JF975005 | JF974691 | JF975263 | | | PERU: depto. Amazonas; E side Río Durañon, ~20 km E Celendín. |

| Taxa | Source | Tissue # | BF7 | COII | ND3 | ND2 | RAGI | RAGII | Locality |
|---|---|---|---|---|---|---|---|---|---|
| *Phacellodomus ruber* | LSUMNS | B26004 | JF974445 | JF975006 | JF974692 | JF975264 | | | PARAGUAY: depto. Presidente Hayes; Estancia Zalazar. |
| *Phacellodomus ferrugineigula* | LSUMNS | B52029 | JF974446 | JF975007 | JF974693 | JF975265 | | | URUGUAY: depto. Rivera; Estancia Trinidad. |
| *Clibanornis dendrocolaptoides* | MPEG | 64811 | JF974447 | JF975008 | JF974694 | JF975266 | JF974851 | JF974822 | BRAZIL: Paraná, Quatro Barras, Corvo. |
| *Anumbius annumbi* | AMNH | DOT12088 | JF974448 | JF975009 | JF974695 | JF975267 | FJ461128 | FJ461030 | ARGENTINA: prov. Buenos Aires; Magdalena, Provincial Route 11, ~14 km. SE Punta Indio. |
| *Coryphistera alaudina* | LSUMNS | B18894 | JF974449 | JF975010 | JF974696 | JF975268 | FJ461129 | FJ461031 | BOLIVIA: depto. Santa Cruz; Cordillera; Estancia Perforación, ~130 km E Charagua. |
| *Siptornis striaticollis* | LSUMNS | B6202 | | JF975011 | JF974697 | JF975269 | FJ461130 | FJ461032 | ECUADOR: prov. Morona-Santiago; W slope Cordillera del Cutucú, S trail from Logroño to Yaupi. |
| *Metopothrix aurantiaca* | LSUMNS | B7367 | | JF975012 | JF974698 | JF975270 | FJ461131 | FJ461033 | PERU: depto. Loreto; Amaz. I. Resario, |

| Taxa | Source | Tissue # | BF7 | COII | ND3 | ND2 | RAGI | RAGII | Locality |
|---|---|---|---|---|---|---|---|---|---|
| | | | | | | | | | 78 km NE Iquitos. |
| *Acrobatornis fonsecai* | LSUMNS | B26330 | | JF975013 | JF974699 | JF975271 | FJ461133 | FJ461035 | BRAZIL: Bahia; Mun. Arataca; above Itatingui. |
| *Xenerpestes minlosi* | LSUMNS | B46627 | | JF975014 | JF974700 | JF975272 | | | PANAMA: prov. Darién; Rancho Frío, ~10 km S El Real. |
| *Xenerpestes singularis* | LSUMNS | B6301 | | JF975015 | JF974701 | JF975273 | FJ461132 | FJ461034 | ECUADOR: prov. Pichincha; Yanacocha, N Slope of Cerro Pichincha. |
| *Premnornis guttuligera* | FMNH | 397999 | JF974450 | JF975016 | JF974702 | JF975274 | FJ461134 | FJ461036 | PERU: depto. Cuzco; Suecia, km 138.5 on Cuzco-Shintuya Highway, Cosñipata Valley. |
| *Premnoplex brunnescens* | AMNH | DOT2675 | JF974451 | JF975017 | JF974703 | JF975275 | FJ461135 | FJ461037 | BOLIVIA: depto. La Paz; prov. Nor Yungas; near Río Elena. |
| *Premnoplex tatei* | IZET-UCV | PT-1 | JF974452 | HM125643 | JF974704 | HM125589 | | | VENEZUELA: Monagas; Cerro Negro, Sierra de Caripe. |
| *Roraimia adusta* | AMNH | DOT11993 | | JF975018 | JF974705 | JF975276 | FJ461136 | FJ461038 | VENEZUELA: Bolivar; La Escalera, km 122 on el Dorado-Santa Helena Rd. |

| Taxa | Source | Tissue # | BF7 | COII | ND3 | ND2 | RAGI | RAGII | Locality |
|---|---|---|---|---|---|---|---|---|---|
| *Margarornis rubiginosus* | AMNH | DOT3673 | JF974453 | JF975019 | JF974706 | JF975277 | FJ461137 | FJ461039 | COSTA RICA: prov. Cartago; 3 km N of Villa Mills-La Georgina. |
| *Margarornis stellatus* | ANSP | 15793 | | JF975020 | JF974707 | JF975278 | | | ECUADOR: prov. Carchi. |
| *Margarornis bellulus* | STRI | GA7 | JF974454 | JF975021 | JF974708 | HM125596 | | | PANAMA: prov. Darién; Serranía de Jungurado, Cerro Antaral, 840m. |
| *Margarornis squamiger* | LSUMNS | B7786 | JF974455 | JF975022 | JF974709 | JF975279 | | | ECUADOR: prov. Pichincha; W slope Andes, SW side Cerro Pichincha. |
| *Pseudoseisura unirufa* | LSUMNS | B38157 | JF974456 | JF975023 | JF974710 | JF975280 | | | BOLIVIA: depto. Santa Cruz; Estancia Cambaras, 38 km SWW San Matías. |
| *Pseudoseisura lophotes* | AMNH | DOT6112 | JF974457 | JF975024 | JF974711 | JF975281 | FJ461138 | FJ461040 | BOLIVIA: depto. Santa Cruz; prov. Cordillera, Izozog, Comunidad Karapari, Estancia San Julián, 1000 m W of Parapet. |
| *Pseudoseisura gutturalis* | LSUMNS | B56811 | JF974458 | JF975025 | JF974712 | JF975282 | | | ARGENTINA: prov. Chubut; ~138 km SSE Esquel on provincial route 19. |
| *Pseudocolaptes* | AMNH | DOT3694 | JF974459 | JF975026 | JF974713 | JF975283 | FJ461139 | FJ461041 | COSTA RICA: Heredia; 3 km N |

| Taxa | Source | Tissue # | BF7 | COII | ND3 | ND2 | RAGI | RAGII | Locality |
|---|---|---|---|---|---|---|---|---|---|
| *lawrencii lawrencii* | | | | | | | | | Porrosati. |
| *Pseudocolaptes lawrencii johnsoni* | LSU | B7801 | JF974460 | JF975027 | JF974714 | JF975284 | | | ECUADOR: prov. El Oro; 9.5 km road to Piñas, 900 m. |
| *Pseudocolaptes boissonneautii* | LSUMNS | B406 | JF974461 | HM125633 | JF974715 | HM125585 | | | PERU: depto. Piura; Cruz Blanca; 33 rd km SW Huancabamba. |
| *Tarphonomus harterti* | LSUMNS | B34573 | JF974462 | JF975028 | JF974716 | JF975285 | FJ461104 | FJ461006 | BOLIVIA: depto. Santa Cruz; Prov. Caballero, Tambo, 14 km SE Camarapa. |
| *Tarphonomus certhioides* | LSUMNS | B18872 | JF974463 | JF975029 | JF974717 | JF975286 | | | BOLIVIA: depto. Santa Cruz; Cordillera; Estancia Perforación ~130 km E Charagua. |
| *Berlepschia rikeri* | FMNH | 391336 | JF974464 | JF975030 | JF974718 | JF975287 | FJ461140 | FJ461042 | BRAZIL: Amapá; Fazenda Itapoã. |
| *Anabacerthia variegaticeps* | LSUMNS | B18075 | JF974465 | JF975031 | JF974719 | JF975288 | | | MEXICO: Oaxaca; Chimalapas, east of Isthmus of Tehuantepec. |
| *Anabacerthia variegaticeps temporalis* | LSUMNS | B12001 | JF974466 | JF975032 | JF974720 | | | | ECUADOR: prov. Esmeraldas; El Placer. |

| Taxa | Source | Tissue # | BF7 | COII | ND3 | ND2 | RAGI | RAGII | Locality |
|---|---|---|---|---|---|---|---|---|---|
| *Anabacerthia striaticollis* | AMNH | DOT2690 | JF974467 | JF975033 | JF974721 | JF975289 | FJ461141 | FJ461043 | BOLIVIA: depto. La Paz; prov. Nor Yungas; near the Río Elena. |
| *Anabacerthia amaurotis* | LSUMNS | B35557 | JF974468 | JF975034 | JF974722 | JF975290 | | | BRAZIL: São Paulo; ~30 km NW Ubatuba. |
| *Syndactyla guttulata* | COP | JP364 | JF974469 | JF975035 | JF974723 | JF975291 | | | VENEZUELA: Monagas; Cerro Piedra de Moler, Serranía del Turimiquire. |
| *Syndactyla subalaris* | LSUMNS | B43483 | JF974470 | JF975036 | JF974724 | JF975292 | | | PERU: depto. San Martin; 24 km ENE Florida. |
| *Syndactyla rufosuperciliata* | LSUMNS | B8051 | JF974471 | JF975037 | JF974725 | JF975293 | FJ461142 | FJ461044 | PERU: depto. Pasco; Playa Pampa, ~8 km NW Cushi on trail to Chaglla. |
| *Syndactyla ruficollis* | LSUMNS | B61318 | JF974472 | JF975038 | JF974726 | JF975294 | | | PERU: depto. Piura; 2 km N Limón de Porculla. |
| *Syndactyla dimidiata* | KU | B150 | JF974473 | JF975039 | JF974727 | JF975295 | | | PARAGUAY: depto. Concepción; San Luis National Park. |
| *Syndactyla roraimae* | LSUMNS | B7410 | JF974474 | JF975040 | JF974728 | JF975296 | JF974852 | JF974823 | VENEZUELA: Amazonas; Cerro de la Neblina base camp. |

| Taxa | Source | Tissue # | BF7 | COII | ND3 | ND2 | RAGI | RAGII | Locality |
|---|---|---|---|---|---|---|---|---|---|
| *Simoxenops ucayalae* | FMNH | 321565 | JF974475 | JF975041 | JF974729 | JF975297 | FJ461143 | FJ461045 | PERU: depto. Cuzco; Tono. |
| *Simoxenops striatus* | LSUMNS | B58428 | JF974476 | JF975042 | JF974730 | JF975298 | | | PERU: depto. Puno; Curva Alegre. |
| *Ancistrops strigilatus* | FMNH | 389820 | JF974477 | JF975043 | JF974731 | JF975299 | FJ461144 | FJ461046 | BRAZIL: Rondônia; Cachoeira Nazaré, W bank Rio Ji-Paraná. |
| *Philydor ruficaudatum* | LSUMNS | B951 | JF974478 | JF975044 | JF974732 | JF975300 | | | BOLIVIA: depto. La Paz; Río Beni, ~20 km by river N Puerto Linares. |
| *Philydor fuscipenne* | LSUMNS | B2250 | JF974479 | JF975045 | JF974733 | JF975301 | | | PANAMA: prov. Darién; ~4 Km along Boca de Cupe trail. |
| *Philydor erythrocercum* | LSUMNS | B6967 | JF974480 | JF975046 | JF974734 | JF975302 | JF974853 | JF974824 | PERU: depto. Loreto; Quebrada Orán, ~5 km N Río Amazonas, 85 km NE Iquitos. |
| *Philydor erythropterum* | LSUMNS | B10571 | JF974481 | JF975047 | JF974735 | JF975303 | | | PERU: depto. Ucayali; W bank Río Shesha, 65 km ENE Pucallpa. |
| *Philydor lichtensteini* | LSUMNS | B25851 | JF974482 | JF975048 | JF974736 | JF975304 | JF974854 | JF974825 | PARAGUAY: depto. Caazapá; Cordillera de Caaguazú. |

| Taxa | Source | Tissue # | BF7 | COII | ND3 | ND2 | RAGI | RAGII | Locality |
|---|---|---|---|---|---|---|---|---|---|
| *Philydor atricapillus* | LSUMNS | B25833 | JF974483 | JF975049 | JF974737 | JF975305 | | | PARAGUAY: depto. Caazapá; Cor. De Caaguazú. |
| *Philydor rufum* | LSUMNS | B40199 | JF974484 | JF975050 | JF974738 | JF975306 | | | PERU: depto. Loreto; ~85 km SE Juanjui. |
| *Philydor pyrrhodes* | AMNH | DOT8864 | EF635329 | EF635348 | EF635367 | JF975307 | FJ461146 | FJ461048 | VENEZUELA: Amazonas; Mrakapiwie. |
| *Anabazenops dorsalis* | LSUMNS | B2046 | JF974485 | JF975051 | JF974739 | HM449828 | | | PERU: depto. Pasco; Puellas, Km 41 on Villa Rica-Puerto Bermudez highway. |
| *Anabazenops fuscus* | FMNH | JMG051 | JF974486 | JF975052 | JF974740 | JF975308 | FJ461147 | FJ461049 | BRAZIL: São Paulo, Intervales. |
| *Cichlocolaptes leucophrus* | MPEG | 64810 | JF974487 | JF975053 | JF974741 | JF975309 | JF974855 | JF974826 | BRAZIL: Paraná; Quatro Barras, Corvo. |
| *Thripadectes ignobilis* | LSUMNS | B11805 | JF974488 | JF975054 | JF974742 | JF975310 | | | ECUADOR: prov. Esmeraldas; El Placer. |
| *Thripadectes rufobrunneus* | AMNH | DOT3651 | EF635330 | EF635349 | EF635368 | JF975311 | FJ461148 | FJ461050 | COSTA RICA: prov. San José; Cerro de la Muerte. |
| *Thripadectes* | LSUMNS | B33493 | JF974489 | JF975055 | JF974743 | JF975312 | | | PERU: depto. Cajamarca; Nuevo Perú, |

| Taxa | Source | Tissue # | BF7 | COII | ND3 | ND2 | RAGI | RAGII | Locality |
|---|---|---|---|---|---|---|---|---|---|
| *melanorhynchus* | | | | | | | | | 16 km NE junction rivers Tabacona and Chinchipe. |
| *Thripadectes holostictus* | LSUMNS | B1650 | JF974490 | JF975056 | JF974744 | JF975313 | | | PERU: depto. Pasco; Santa Cruz, ~9 km SSE Oxapampa. |
| *Thripadectes virgaticeps* | LSUMNS | B7798 | JF974491 | JF975057 | JF974745 | JF975314 | | | ECUADOR: prov. Pichincha; SW slope Cerro Pichincha, on road to Mindo. |
| *Thripadectes flammulatus* | ANSP | 15758 | JF974492 | JF975058 | JF974746 | JF975315 | | | ECUADOR: prov. Carchi. |
| *Thripadectes scrutator* | LSUMNS | B1885 | JF974493 | JF975059 | JF974747 | JF975316 | | | PERU: depto. Pasco; Cumbre de Ollón, ~12 km E Oxapampa. |
| *Hyloctistes subulatus subulatus* | AMNH | DOT3867 | JF974494 | JF975060 | JF974748 | | FJ461145 | FJ461047 | VENEZUELA: Amazonas; Río Mawarinuma, Cerro de la Neblina base camp. |
| *Hyloctistes subulatus assimilis* | LSUMNS | B11744 | JF974495 | JF975061 | JF974749 | JF975317 | | | ECUADOR: prov. Esmeraldas; El Placer. |
| *Automolus ochrolaemus* | LSUMNS | B28036 | JF974496 | JF975062 | JF974750 | HM449831 | | | PERU: depto. Loreto; 77 km WNW |

| Taxa | Source | Tissue # | BF7 | COII | ND3 | ND2 | RAGI | RAGII | Locality |
|---|---|---|---|---|---|---|---|---|---|
| | | | | | | | | | Contamana. |
| *Automolus infuscatus* | LSUMNS | B4283 | JF974497 | JF975063 | JF974751 | HM449829 | | | PERU: depto. Loreto; Lower Río Napo region, E bank Río Yanayacu, 90 km N Iquitos. |
| *Automolus paraensis* | LSUMNS | B35334 | JF974498 | JF975064 | JF974752 | JF975318 | | | BRAZIL: Pará; E bank of Rio Teles Pires, 4 km up river from mouth of Rio São Benedito. |
| *Automolus lammi* | FMNH | 399211 | JF974499 | JF975065 | JF974753 | | | | BRAZIL: Alagoas; Ibateouara, Engenho Ceimba, Usina Serra Grande. |
| *Automolus leucophthalmus* | LSUMNS | B25867 | JF974500 | JF975066 | JF974754 | JF975319 | | | PARAGUAY: depto. Caazapá; Cor. de Caaguazú, 7.5 km E. San Carlos. |
| *Automolus melanopezus* | LSUMNS | B8972 | JF974501 | JF975067 | JF974755 | HM449830 | | | BOLIVIA: depto. Pando; Prov. Nicolás Suarez; ~12 km by road S Cobija, ~8 km W on road to Mucden. |
| *Automolus rubiginosus saturatus* | LSUMNS | B2234 | JF974502 | JF975068 | JF974756 | | JF974856 | JF974827 | PANAMA: prov. Darién; Cana, 2133 m. |

| Taxa | Source | Tissue # | BF7 | COII | ND3 | ND2 | RAGI | RAGII | Locality |
|---|---|---|---|---|---|---|---|---|---|
| *Automolus rubiginosus nigricauda* | LSUMNS | B11807 | JF974503 | JF975069 | JF974757 | | | | ECUADOR: prov. Esmeraldas; El Placer. |
| *Automolus rubiginosus watkinsi* | LSUMNS | B10684 | JF974504 | JF975070 | JF974758 | | | | PERU: depto. Ucayali; W bank Río Shesha, ca. 65 km ENE Pucallpa. |
| *Automolus rufipectus* | Andes-O | 433 | | JF975071 | JF974759 | JF975320 | | | COLOMBIA: depto. Magdalena; Santa Marta, Cerro San Lorenzo, Vista Nieve. |
| *Automolus rufipileatus* | LSUMNS | B1074 | JF974505 | JF975072 | JF974760 | JF975321 | JF974857 | JF974828 | BOLIVIA: depto. La Paz; Río Beni, ~20 km by river N Puerto Linares. |
| *Hylocryptus erythrocephalus* | LSUMNS | B61296 | JF974506 | JF975073 | JF974761 | JF975322 | JF974858 | JF974829 | PERU: depto. Lambayeque; Quebrada Caballito, 3 km NE El Tocto. |
| *Hylocryptus rectirostris* | KU | 3567 | JF974507 | JF975074 | JF974762 | JF975323 | | | PARAGUAY: depto. Concepción; Arroyo Tagatiya-Mi. |
| *Lochmias nematura* | AMNH | DOT12074 | EF635332 | EF635351 | EF635370 | JF975324 | FJ461151 | FJ461053 | ARGENTINA: prov. Misiones; Parque Provincal Urugua-í, ~1 km W park headquarters, Provincial Route 19. |
| *Heliobletus* | FMNH | 389197 | JF974508 | JF975075 | JF974763 | JF975325 | FJ461152 | FJ461054 | BRAZIL: São Paulo; Boracéia |

| Taxa | Source | Tissue # | BF7 | COII | ND3 | ND2 | RAGI | RAGII | Locality |
|---|---|---|---|---|---|---|---|---|---|
| *contaminatus* | | | | | | | | | Biological Station, Salesópolis. |
| *Microxenops milleri* | LSUMNS | B4505 | JF974509 | JF975076 | JF974764 | JF975326 | FJ461154 | FJ461056 | PERU: depto. Loreto; Lower Río Napo region, E bank Río Yanayacu, 90 km N Iquitos. |
| *Xenops tenuirostris* | LSUMNS | B5027 | JF974510 | JF975077 | JF974765 | JF975327 | | | PERU: depto. Loreto; S Río Amazonas, ~10km SSW mouth Río Napo on E bank Quebrada Vainilla. |
| *Xenops minutus remoratus* | AMNH | DOT8845 | JF974511 | JF975078 | JF974766 | JF975328 | FJ461153 | FJ461055 | VENEZUELA: Amazonas; Mrakapiwie. |
| *Xenops minutus littoralis* | LSUMNS | B11948 | JF974512 | JF975079 | JF974767 | JF975329 | | | ECUADOR: prov. Esmeraldas; El Placer. |
| *Xenops minutus minutus* | LSUMNS | B25938 | JF974513 | JF975080 | JF974768 | JF975330 | | | PARAGUAY: depto. Caaguazú; Cord. de Caaguazú, 7.5 km E San Carlos. |
| *Xenops rutilans* | LSUMNS | B5436 | JF974514 | JF975081 | JF974769 | JF975331 | | | PERU: depto. San Martín; 20 km by road NE Tarapoto on road to Yurimaguas. |

| Taxa | Source | Tissue # | BF7 | COII | ND3 | ND2 | RAGI | RAGII | Locality |
|---|---|---|---|---|---|---|---|---|---|
| *Megaxenops parnaguae* | LGEMA | P2287 | JF974515 | JF975082 | JF974770 | JF975332 | JF974859 | JF974830 | BRAZIL: Piauí; Parque Nacional Serra das Confusões. |
| *Pygarrhichas albogularis* | AMNH | DOT9930 | JF974516 | JF975083 | JF974771 | JF975333 | FJ461156 | FJ461058 | ARGENTINA: prov. Río Negro; Bariloche. |
| *Dendrocincla tyrannina* | LSUMNS | B1743 | JF974517 | JF975084 | JF974772 | JF975334 | | | PERU: depto. Pasco; Santa Cruz, ~9 Km SSE Oxapampa. |
| *Dendrocincla fuliginosa* | AMNH | DOT12706 | GQ906727 | GQ906741 | GQ922582 | GQ906712 | FJ461157 | FJ460973 | VENEZUELA: edo. Amazonas; Río Baria, Cerro de la Neblina, base camp. |
| *Dendrocincla anabatina* | LSUMNS | B17144 | JF974518 | JF975085 | JF974773 | JF975335 | | | BELIZE: Toledo; Forestry Camp (Salamanca), 1 km NNE. |
| *Dendrocincla merula* | LSUMNS | B2722 | JF974519 | JF975086 | JF974774 | JF975336 | | | PERU: depto. Loreto; 1 km N Río Napo, 157 km by river NNE Iquitos. |
| *Dendrocincla homochroa* | LSUMNS | B19281 | JF974520 | JF975087 | JF974775 | JF975337 | | | MEXICO: Oaxaca; Chimalapas, east of Isthmus of Tehuantepec. |
| *Deconychura longicauda* | LSUMNS | B4753 | JF974521 | JF975088 | JF974776 | JF975338 | FJ461158 | FJ460974 | PERU: depto. Loreto; S Río Amazonas, ~10km SSW mouth Río Napo on E bank |

| Taxa | Source | Tissue # | BF7 | COII | ND3 | ND2 | RAGI | RAGII | Locality |
|---|---|---|---|---|---|---|---|---|---|
| | | | | | | | | | Quebrada Vainilla. |
| *Certhiasomus stictolaemus* | LSUMNS | B27420 | JF974522 | JF975089 | JF974777 | JF975339 | JF974860 | JF974831 | PERU: depto. Loreto; NE bank upper Río Cushabatay, 84 km WNW Contamana. |
| *Sittasomus griseicapillus* | LSUMNS | B22699 | JF974523 | JF975090 | AY089894 | AY089834 | | | BOLIVIA: depto. La Paz; Prov. B. Saavedra, 83 km by road E Charazani, Cerro Asunta Pata. |
| *Glyphorynchus spirurus* | AMNH | DOT4274 | JF974524 | JF975091 | JF974778 | JF975340 | FJ461160 | FJ460976 | VENEZUELA: Amazonas; Sierra de Tapirapeco, Cerro Tamacuari. |
| *Drymotoxeres pucherani* | LSUMNS | B34815 | GQ906735 | GQ906749 | GQ922590 | GQ906721 | JF974861 | JF974832 | PERU: depto. Cajamarca; Cordillera del Cóndor, Picorana. |
| *Drymornis bridgesii* | LSUMNS | B25799 | JF974525 | AY489488 | JF974779 | GQ906713 | FJ461161 | FJ460977 | PARAGUAY: depto. Alto Paraguay; Madrejón. |
| *Nasica longirostris* | LSUMNS | B4491 | GQ906728 | GQ906742 | GQ922583 | GQ906714 | JF974862 | JF974833 | PERU: depto. Loreto; Lower Río Napo region, E bank Río Yanayacu, 90 km N Iquitos. |

| Taxa | Source | Tissue # | BF7 | COII | ND3 | ND2 | RAGI | RAGII | Locality |
|---|---|---|---|---|---|---|---|---|---|
| *Dendrexetastes rufigula* | FMNH | 389815 | GQ906729 | GQ906743 | GQ922584 | GQ906715 | JF974863 | JF974834 | BRAZIL: Rondônia; Cachoeira Nazaré, W bank Rio Ji-Paraná. |
| *Hylexetastes stresemanni* | LSUMNS | B9111 | JF974526 | JF975092 | JF974780 | JF975341 | | | BOLIVIA: depto. Pando; Prov. Nicolás Suarez; ~12 km by road S Cobija, ~8 km W on road to Mucden. |
| *Hylexetastes perrotii* | FMNH | 392022 | GQ906730 | GQ906744 | GQ922585 | GQ906716 | FJ461164 | FJ460980 | BRAZIL: Mato Grosso: Alta Floresta, upper Rio Teles Pires, Rio Cristalino lodge. |
| *Xiphocolaptes promeropirhynchus* | LSUMNS | B34831 | JF974527 | JF975093 | JF974781 | JF975342 | | | PERU: depto. Cajamarca; Cordillera del Cóndor; Picorana. |
| *Xiphocolaptes falcirostris* | LGEMA | P2333 | JF974528 | JF975094 | JF974782 | JF975343 | | | BRAZIL: Piauí; Parque Nacional Serra das Confusões. |
| *Xiphocolaptes albicollis* | LSUMNS | 25944 | JF974529 | JF975095 | JF974783 | JF975344 | | | PARAGUAY: depto. Caazapá; Cordillera de Caaguazú, 7.5 km E San Carlos. |
| *Xiphocolaptes major* | AMNH | DOT2194 | GQ906731 | GQ906745 | GQ922586 | GQ906717 | FJ461165 | FJ460981 | BOLIVIA: depto. Santa Cruz; prov. |

| Taxa | Source | Tissue # | BF7 | COII | ND3 | ND2 | RAGI | RAGII | Locality |
|---|---|---|---|---|---|---|---|---|---|
| | | | | | | | | | Cordillera, Izozog, Comunidad Karapari, Estancia San Julián, 1000 m W of Parapet. |
| *Dendrocolaptes sanctithomae* | AMNH | DOT3689 | GQ906732 | GQ906746 | GQ922587 | GQ906718 | JF974864 | JF974835 | COSTA RICA: prov. Puntarenas; 0.8 km NW Cuatro Cruces on Route 1. |
| *Dendrocolaptes certhia certhia* | LSUMNS | B48421 | JF974530 | JF975096 | JF974784 | JF975345 | | | GUYANA: Kopinang Mountain, ~7 km SW Kopinang Village. |
| *Dendrocolaptes certhia concolor* | LSUMNS | B18125 | JF974531 | JF975097 | JF974785 | JF975346 | | | BOLIVIA: depto. Santa Cruz; Velasco, Parque Nacional Noel Kempff Mercado. |
| *Dendrocolaptes picumnus* | LSUMNS | B9282 | JF974532 | JF975098 | JF974786 | JF975347 | | | BOLIVIA: depto. Pando; Prov. Nicolás Suarez; ~12 km by road S Cobija, ~8 km W on road to Mucden. |
| *Dendrocolaptes hoffmannsi* | LSUMNS | B25420 | JF974533 | JF975099 | JF974787 | JF975348 | | | BRAZIL: Amazonas; ~6 km E Borba on "Puxurizal" road. |
| *Dendrocolaptes platyrostris* | LSUMNS | B25952 | JF974534 | JF975100 | JF974788 | JF975349 | | | PARAGUAY: depto. Caazapá; Cordillera de Caaguazú, 7.5 km E San |

| Taxa | Source | Tissue # | BF7 | COII | ND3 | ND2 | RAGI | RAGII | Locality |
|---|---|---|---|---|---|---|---|---|---|
| | | | | | | | | | Carlos. |
| *Dendroplex picus* | FMNH | 334433 | JF974535 | JF975101 | JF974789 | JF975350 | FJ461167 | FJ460983 | BOLIVIA: depto. Beni; Laguna Suárez, 5 km SW Trinidad. |
| *Dendroplex kienerii* | LSUMNS | B25413 | JF974536 | JF975102 | JF974790 | JF975351 | | | BRAZIL: Amazonas; Rio Amazonas, Ilha do Careiro, ~20 km E Manaus. |
| *Xiphorhynchus obsoletus* | LSUMNS | B4396 | JF974537 | JF975103 | JF974791 | JF975352 | | | PERU: depto. Loreto; Lower Río Napo region, E bank Río Yanayacu, 90 km N Iquitos. |
| *Xiphorhynchus fuscus* | LSUMNS | B35576 | GQ906733 | GQ906747 | GQ922588 | GQ906719 | JF974865 | JF974836 | BRAZIL: Bahia; ~16 km W Porto Seguro RPPN Vera Cruz. |
| *Xiphorhynchus ocellatus* | LSUMNS | B35598 | JF974538 | JF975104 | JF974792 | JF975353 | | | BRAZIL: Pará; ~139 km WSW Santarém, W of Rio Tapajos and Alto Rio Arapiuns. |
| *Xiphorhynchus chunchotambo* | LSUMNS | B22631 | JF974539 | JF975105 | JF974793 | JF975354 | | | BOLIVIA: depto. La Paz; Prov. B. Saavedra, 83 km by road E Charazani, Cerro Asunta Pata. |

| Taxa | Source | Tissue # | BF7 | COII | ND3 | ND2 | RAGI | RAGII | Locality |
|---|---|---|---|---|---|---|---|---|---|
| *Xiphorhynchus elegans* | LSUMNS | B31384 | JF974540 | JF975106 | JF974794 | AY089852 | | | BRAZIL: Rondônia; ~90 km E of Vila Nova Mamoré. |
| *Xiphorhynchus spixii* | LSUMNS | B35542 | JF974541 | JF975107 | JF974795 | JF975355 | | | BRAZIL: Pará; Fazenda Morelândia, 8 km N of Santa Bárbara do Pará. |
| *Xiphorhynchus pardalotus* | LSUMNS | B35635 | JF974542 | JF975108 | JF974796 | AY089848 | | | BRAZIL: Pará; baixo Rio Curuá, N. of Amazon River, ~30 km N. Curuá, Pacoval Village. |
| *Xiphorhynchus susurrans* | LSUMNS | B26942 | JF974543 | JF975109 | JF974797 | JF975356 | | | PANAMA: prov. Panamá; Old Gamboa Road, 5 km NW Paraiso. |
| *Xiphorhynchus guttatus* | LSUMNS | B35582 | JF974544 | JF975110 | JF974798 | AY089869 | | | BRAZIL: Bahia; ~16 km W Porto Seguro RPPN Vera Cruz. |
| *Xiphorhynchus guttatus eytoni* | LSUMNS | B35546 | JF974545 | JF975111 | JF974799 | AY089845 | | | BRAZIL: Pará; Fazenda Morelândia, 8 km N of Santa Bárbara do Pará. |
| *Xiphorhynchus flavigaster* | LSUMNS | B8743 | JF974546 | JF975112 | JF974800 | JF975357 | JF974866 | JF974837 | BELIZE: Toledo; Forestry Camp (Salamanca), 1 km NNE. |
| *Xiphorhynchus* | LSUMNS | B26581 | JF974547 | JF975113 | JF974801 | JF975358 | | | PANAMA: prov. Colón; 17 km by road |

| Taxa | Source | Tissue # | BF7 | COII | ND3 | ND2 | RAGI | RAGII | Locality |
|---|---|---|---|---|---|---|---|---|---|
| *lachrymosus* | | | | | | | | | NW Gamboa, Río Agua Salud. |
| *Xiphorhynchus erythropygius* | LSUMNS | B28185 | JF974548 | JF975114 | JF974802 | AY089858 | | | PANAMA: prov. Chiriquí; Dist. Gualaca; Cordillera Central, 4.3 km by road S Lago Fortuna dam. |
| *Xiphorhynchus triangularis* | LSUMNS | B34817 | JF974549 | JF975115 | JF974803 | JF975359 | | | PERU: depto. Cajamarca; Cordillera del Condor; Picorana. |
| *Lepidocolaptes souleyetii* | LSUMNS | B16084 | JF974550 | JF975116 | JF974804 | | | | COSTA RICA: prov. Puntarenas; Río Agujas, 1 km from river mouth. |
| *Lepidocolaptes angustirostris* | LSUMNS | B18768 | JF974551 | JF975117 | JF974805 | AY089838 | | | BOLIVIA: depto. Santa Cruz; Cordillera; Estancia Perforación, ~130 km E Charagua. |
| *Lepidocolaptes leucogaster* | MBM | 12905 | JF974552 | JF975118 | JF974806 | JF975360 | | | MEXICO: Jalisco, Sierra Bolaños. |
| *Lepidocolaptes affinis* | LSUMNS | B19834 | JF974553 | JF975119 | JF974807 | JF975361 | | | COSTA RICA: prov. Cartago; 3 km ENE Villa Mills, km 98 Pan American Hwy. |

| Taxa | Source | Tissue # | BF7 | COII | ND3 | ND2 | RAGI | RAGII | Locality |
|---|---|---|---|---|---|---|---|---|---|
| *Lepidocolaptes lacrymiger* | AMNH | DOT7051 | GQ906734 | GQ906748 | GQ922589 | GQ906720 | FJ461168 | FJ460984 | BOLIVIA: depto. La Paz; Parque Nacional Apolobamba. |
| *Lepidocolaptes falcinellus* | LSUMNS | B52019 | JF974554 | JF975120 | JF974808 | JF975362 | | | URUGUAY: depto. Cerro Largo; Sierra de los Ríos, Paso Las Cañas. |
| *Lepidocolaptes albolineatus* | LSUMNS | B18457 | JF974555 | JF975121 | JF974809 | AY089865 | | | BOLIVIA: depto. Santa Cruz; Velasco, Parque Nacional Noel Kempff Mercado, 86 km ESE Florida. |
| *Campylorhamphus trochilirostris* | AMNH | DOT2234 | GQ906736 | GQ906750 | GQ922591 | GQ906722 | JF974867 | JF974838 | BOLIVIA: depto. Santa Cruz; prov. Cordillera, Izozog, Comunidad Karapari, Estancia San Julian, 1000 m W of Parapetí. |
| *Campylorhamphus falcularius* | LGEMA | 1529 | GQ906737 | GQ906751 | GQ922592 | GQ906723 | | | BRAZIL: São Paulo; Estação Ecológica Itaberá. |
| *Campylorhamphus procurvoides* | LSUMNS | B7501 | GQ906738 | GQ906752 | GQ922593 | GQ906724 | | | VENEZUELA: Amazonas; Cerro de la Neblina, base camp. |
| *Campylorhamphus* | LSUMNS | B33216 | GQ906739 | GQ906753 | GQ922594 | GQ906725 | | | PERU: depto. Cajamarca; ~3 km NNE |

| Taxa | Source | Tissue # | BF7 | COII | ND3 | ND2 | RAGI | RAGII | Locality |
|---|---|---|---|---|---|---|---|---|---|
| *pusillus* | | | | | | | | | San José de Lourdes. |
| *Formicarius colma* | | | AY489454 | AY489504 | AY489552 | AY370587 | AY056993 | AY443147 | |
| *Melanopareia torquata* | | | GU371839 | AY489505 | AY489553 | JF975363 | FJ461228 | FJ461002 | |
| *Terenura sharpei* | | | GU371842 | GU371846 | EF640122 | EF640055 | FJ461190 | FJ461080 | |
| *Tyrannus melancholicus* | | | AY489417 | AF132614 | AF132641 | DQ294576 | AF143739 | AY443243 | |
| *Tityra semifasciata* | | | AY489426 | AY489476 | AY489524 | DQ363967 | AY443337 | AY443237 | |

AMNH – American Museum of Natural History, New York City, USA; ANSP – Academy of Natural Sciences, Philadelphia, USA; FMNH – Field Museum of Natural History, Chicago, USA; ICN – Instituto de Ciencias Naturales, Universidad Nacional de Colombia, Bogotá, Columbia; LSUMNS – Louisiana State University Museum of Natural Science, Baton Rouge, USA; USNM – National Museum of Natural History, Smithsonian Institution, Washington, DC, USA; COP – Colección Ornitológica Phelps, Caracas, Venezuela; IZET-UCV – Instituto de Zoología y Ecología Tropical, Universidad Central de Venezuela; KU – University of Kansas Biodiversity Research Center, Lawrence, USA; CUMV – Cornell University Museum of Vertebrates, Ithaca, USA; LGEMA – Laboratório de Genética e Evolução Molecular de Aves, Universidade de São Paulo (São Paulo, Brazil); MBM – Marjorie Barrick Museum (Las Vegas, USA); MCN - Coleção Ornitológica, Museu de Ciências Naturais, Fundação Zoobotânica do Rio Grande do Sul (Porto Alegre, Brazil); MPEG – Coleção Ornitológica do Museu Paraense Emílio Goeldi (Belém, Brazil); STRI – Instituto Smithsonian de Investigaciones Tropicales, Panamá; Andes-O – Museo de Historia Natural, Ornithology Section, Universidad de los Andes, Bogotá, Colombia; UFMGDZ – Coleção Ornitológica do Departamento de Zoologia da Universidade Federal de Minas Gerais, Belo Horizonte, MG, Brazil; UFMG - Laboratório de Biodiversidade e Evolução Molecular da Universidade Federal de Minas Gerais, Belo Horizonte, MG, Brazil

**Table S2. Statistics for selection of the best partitioning strategy.**

| Model | No. Partitions | No. Parameters | AICc[a] | ΔAIC[b] |
|---|---|---|---|---|
| **GTR+ Γ+I** | **16** | **112** | 284258 | 0 |
| GTR+ Γ+I | 14 | 98 | 284385 | 126 |
| GTR+ Γ+I | 11 | 77 | 284770 | 512 |
| GTR+ Γ+I | 9 | 63 | 284812 | 553 |
| GTR+ Γ+I | 7 | 49 | 284776 | 518 |
| GTR+ Γ+I | 4 | 28 | 286184 | 1926 |
| GTR+ Γ+I | 2 | 14 | 288947 | 4689 |
| GTR+ Γ | 16 | 96 | 284645 | 387 |
| GTR+ Γ | 14 | 84 | 284796 | 538 |
| GTR+ Γ | 11 | 66 | 285276 | 1018 |
| GTR+ Γ | 9 | 54 | 285519 | 1261 |
| GTR+ Γ | 7 | 42 | 285506 | 1248 |
| GTR+ Γ | 4 | 24 | 286271 | 2013 |
| GTR+ Γ | 2 | 12 | 289669 | 5411 |

[a]Small sample size version of the Akaike Information Criterion

[b]Difference in AIC scores between each model and the overall best-fit model.